CHALMERS

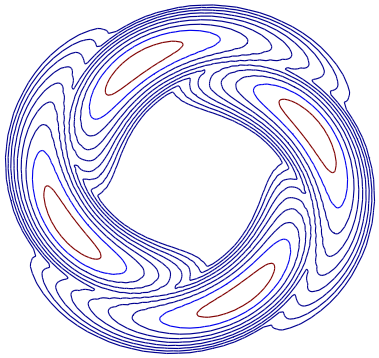

Coded Modulation Techniques in Fiber-Optical Communications

Lotfollah Beygi

Department of Signals and Systems
Communication Systems Group
CHALMERS UNIVERSITY OF TECHNOLOGY
Gothenburg, Sweden 2010

Thesis for the degree of Licentiate of Engineering

Coded Modulation Techniques in Fiber-Optical Communications

Lotfollah Beygi

CHALMERS

Communication Systems Group
Department of Signals and Systems
Chalmers University of Technology

Gothenburg 2010

Lotfollah Beygi
Coded Modulation Techniques
in Fiber-Optical Communications.

Department of Signals and Systems
Technical Report No. R015/2010
ISSN 1403-266X

Communication Systems Group
Department of Signals and Systems
Chalmers University of Technology
SE-412 96 Gothenburg, Sweden
Telephone: + 46 (0)31-772 1000

Front cover illustration: The joint probability density function of the received amplitude and phase of one polarization for a dual-polarization system (see [Paper D] for details).

This thesis has been prepared using LaTeX.

Printed by Chalmers Reproservice,
Gothenburg, Sweden, November 2010.

To Maryam

Abstract

Today's high demand for increasing the data transmission rate motivates a great challenge to improve the spectral efficiency of fiber-optical channels. In order to achieve a higher spectral efficiency, exploiting an advanced coded modulation scheme is inevitable. Since a general fiber-optic link is a non-Gaussian channel with nonlinear behavior, new coded modulation schemes need to be designed for these non-Gaussian channels. The performance of many binary classic codes such as Reed-Solomon and capacity-achieving codes such as low density parity-check codes and turbo codes, originally designed for the additive white Gaussian noise channel (AWGN), has been evaluated in fiber-optical channels. However, the design of error-correcting codes for such a non-Gaussian fiber-optical channel is complicated and is not well investigated in the literature.

Multilevel coded modulation (MLCM) uses low complexity multistage decoding, which is a suitable structure for a very high-rate fiber-optical communication system. We propose a new rate-allocation method for the MLCM scheme [Paper A] based on the minimization of the total block error rate. The proposed approach uses Reed–Solomon component codes and hard decision multistage decoding.

A multidimensional MLCM system with an N-dimensional constellation constructed from the Cartesian product of N identical one-dimensional constellations is introduced in [Paper B]. According to our analysis, the multidimensional scheme shows better trade-off between complexity and performance than a one-dimensional MLCM. Exploiting the results in Papers A and B, we present a novel MLCM scheme for a non-Gaussian dispersion-managed fiber channel [Paper C]. This MLCM scheme is designed with a ring constellation and nonlinear post-compensation of the self-phase modulation produced via the Kerr effect. In this scheme, a new set partitioning based on the Ungerboeck approach is introduced to maintain unequal error protection in amplitude and phase. In contrast to AWGN channels, increasing the minimum Euclidean distance is not a valid criterion to design a coded system for such fiber-optical channels.

Finally, the joint probability density function of the received amplitudes and phases of a dispersion-managed fiber-optical channel is derived in [Paper D]. This analysis is performed for dual-polarization transmission with both lumped and distributed amplifications. The derived statistics can be used to design an ML receiver for data transmission systems in these channels.

Keywords:
Dual polarization, fiber-optical communications, multilevel coded modulation, multidimensional set partitioning, nonlinear phase noise, rate allocation, signal statistics of nonlinear phase noise, self-phase modulation

List of Publication

Appended papers

This thesis is based on the following papers:

[A] L. Beygi, E. Agrell, M. Karlsson, and B. Makki, "A Novel Rate Allocation Method for Multilevel Coded Modulation," *in Proceedings of IEEE International Symposium on Information Theory*, pp. 1983–1987, June 2010.

[B] L. Beygi, E. Agrell, and M. Karlsson, "On the Dimensionality of Multilevel Coded Modulation in the High SNR Regime," *IEEE Communications Letters*, vol. 14, no. 11, pp.1056–1058, Nov. 2010.

[C] L. Beygi, E. Agrell, P. Johannisson, and M. Karlsson, "A Novel Multilevel Coded Modulation Scheme for Fiber Optical Channel with Nonlinear Phase Noise," *in Proceedings of IEEE Global Communications Conference*, Dec. 2010 (to appear).

[D] L. Beygi, E. Agrell, M. Karlsson, and P. Johannisson, "Signal Statistics in Fiber-Optical Channels with Dual Polarization and Self-Phase Modulation," submitted to *IEEE Signal Processing Letters*, Nov. 2010.

Contents

Acknowledgements

First of all, I am heartily thankful to professor Erik Agrell, for his support, guidance, and patience from the initial to this level that enabled me to develop an understanding of the subject. His profound knowledge in digital communication specially in coding theory and his scientific curiosity are a constant source of inspiration for me during this research. I am also very grateful to have Professor Magnus Karlsson as my co-supervisor. I benefited tremendously from his numerous creative thinkings and fruitful discussions.

Interacting with FORCE members consist of people from S2 and MC2 departments gave me a great opportunity to speed up my research and broaden my perspective on all aspects of fiber-optical communications. I would like to thank Pontus Johannisson. His clarity of thought and keen insight have greatly influenced my understanding from different impairment in a fiber-optical channel.

I would like to give thanks to Prof. Erik Ström for providing an enthusiastic research environment in the Communication Systems and Information Theory group. I am indebted to many of the current and former members of the communication system group at Chalmers. In particular, I want to thank Arash, Mohammad, Behrooz, Ali, Johnny, Guillermo and Nima for being open to discuss my questions, Kasra for saturating me with all types of information, academic and non-academic, Alex for discussion about coded modulation and being a kind roommate, and Dr. Stylianos for helping me a lot in IT++ and linux.

I am grateful to Prof. Arne Svensson and Dr. Thomas Ericsson for very helpful discussion in PhD courses and all people who have helped and inspired me during my doctoral study. For helping me with administrative tasks related to this thesis, I send my gratitude to Agneta and Natasha. I would like to thank Lars Börjesson for the computer and software support.

Last but not the least, my deepest gratitude goes to my family for their unflagging love and support throughout my life; this work is simply impossible without them.

This work has been supported by the Swedish Research Council (VR) under Grant 2007-6223.

Lotfollah Beygi
Göteborg, November, 2010

Acronyms

AWGN:	Additive White Gaussin Noise
bps:	bit per second
PSK:	Phase Shift Keying
PAM:	Pulse Amplitude Modulation
QAM:	Quadrature Amplitude Modulation
PDF:	Probability Density Function
TCM:	Trellis Coded Modulation
MLCM:	Multi-Level Coded Modulation
BICM:	Bit-Interleaved Coded Modulation
MED:	Minimum Euclidean Distance
MEBD:	Minimum Euclidean Block Distance
SNR:	Signal-to-Noise Ratio
MSD:	Multi-Stage Decoding
PDL:	Parallel independent Decoding of the individual Layers
CM:	Coded Modulation
BDL:	Balance Distance Rule
BLER:	Block Error Rate
SMF:	Single Mode Fiber
DCF:	Dispersion Compensation Fiber
NLSE:	Non-Linear Schrödinger Equation
NRZ:	Non-Return to Zero
ASE:	Amplified Spontaneous Emission
MAP:	Maximum A posteriori Probability
ML:	Maximum Likelihood
BEC:	Binary Erasure Channel
BSC:	Binary Symmetric Channel
BCH:	Bose-Chaudhuri-Hocquenghem
LDPC:	Low Density Parity-Check
IQM:	I/Q Modulator
LMM:	Lagrange Multiplier Method
CDR:	Capacity Design Rule

Chapter 1

Introduction

Digital communication has attained a vital role in the infrastructure of modern society, from multimedia broadcasting to advanced military communication systems. The foundation of rapidly growing information technology, one of the greatest engineering achievements of the twentieth century, was begun by Shannon [1] in 1948. According to his theorem, data transmission over a noisy channel is possible with an arbitrarily chosen low error rate at finite signal power as long as the transmission rate (coding rate) is not greater than a certain constant, called the capacity of the channel. Conversely, error-free transmission is impossible if one uses a transmission rate which exceeds the capacity of the channel, regardless of the exploited transmission scheme. However, Shannon did not introduce any practical approach to designing such a capacity achieving system. Since then, tremendous efforts were initiated to devise appropriate schemes for practical implementation.

In the design of a data transmission system, the required power, spectrum bandwidth, and complexity for a reliable transmission need to be taken into account. Much effort was devoted to optimizing these factors simultaneously. However, there is always a trade-off in fulfilling all these parameters together.

Among different available data transmission systems, fiber-optical communication systems have introduced significant changes in the telecommunications industries. These systems were first developed in the 1970s and they have played a major role in the drastic development of information technology. Due to their superiorities over electrical transmission systems, optical fibers have extensively replaced copper wire links in networks. As the demand for higher rates continues to increase rapidly at about 60% per year [2], many studies on the capacity of optical networks have been presented (see [3] and references therein).

Traditional error correcting coding manipulates the information bits and adds some parity bits in order to recover these bits after receiving them with some errors. Such coding methods were introduced in the mid-1990s for fiber channels, typically using 7% redundancy (parity) bits. However, codes with higher redundancy (on the order of 25%) have mostly been used in long-haul systems so far. In these schemes, coding and modulation units operate independently.

The superiority of applying join channel coding and modulation scheme to increase the performance of a system was already known in the 1960s [4]. The combination of modulation and convolutional codes with soft Viterbi decoding was introduced by Ungerboeck [5]. In his pioneering work [6], he suggested a concept of set partitioning of a signal set in a so-called trellis coded modulation (TCM) scheme. Set partitioning means splitting a signal set into smaller subsets by increasing the minimum Euclidean

distance (MED) within the subsets. Independently, Imai and Hirakawa [7] proposed a multilevel coded modulation (MLCM) scheme based on multistage decoding. The idea behind MLCM is to convert a single channel with multilevel modulation format to some parallel channels with binary inputs. These parallel channels corresponding to the particular binary labeling (set partitioning) need different error protections (code rates). The MLCM scheme proposed unequal error protection of the parallel channels; e.g., the channel with higher capacity should be protected by higher rate code.

The main aim of this report is to design a coded modulation scheme for a fiber optical channel. In general, a fiber channel is a non-Gaussian channel, and there is no standard design framework for a coded modulation scheme in the literature for such channels. The well investigated MLCM techniques need to be adapted or redesigned for this new channel; e.g., maximizing the MED of the system is not a valid criterion anymore for this channel, even in high signal-to-noise ratio (SNR).

To facilitate the understanding of the included contributions in this report, we first exploit a unified scheme to describe coded modulation techniques [8–10] for the additive white Gaussian noise (AWGN) channel in Chapter 2. With special interest for an optical link, we describe an MLCM scheme and its extension to multidimensional signal sets. Multidimensional MLCM shows better trade-off between complexity and performance in comparison to one-dimensional MLCM.

A general model of a fiber optical channel is investigated in Chapter 3. Statistics of the received signal in a dispersion-managed fiber link are also studied to introduce compensation techniques based on electronic digital signal processing. In Chapter 4, after reviewing proposed data transmission systems for a fiber optical channel with different impairments, a new coded modulation scheme is introduced for a non-Gaussian channel. Finally, Chapter 5 concludes the discussion and introduces some open problems in the field for future study.

Chapter 2

Coded modulation in additive white Gaussian noise channels

1 Introduction

Coded modulation is a joint coding and modulation scheme which considers the impairments of a channel. One advantage of coded modulation is that the joint design gives us more freedom in optimizing the total performance of the system. The combination of a bandwidth efficient modulation format and a forward error correcting code can achieve coding gain without bandwidth expansion or reducing data rate. The redundancy needed for error control codes comes from constellation expansion. This technique has had applications in band-limited channels such as voiceband telephone, terrestrial microwave, satellite and mobile channels [11–14].

Traditional approaches in the design of coded modulation systems were focused on the minimum Euclidean distance (MED) and asymptotic gains [7, 15], while exploiting techniques from information theory have changed these design criteria [16]. It is proved in [17] that multilevel coded modulation (MLCM) together with multistage decoding (MSD) suffices to approach the Shannon channel [1] capacity if the component code rates are properly chosen.

In fact, not only MED of the generated symbol sequences plays an important role in the performance of a system with multilevel modulation format, but neighboring coefficients [18] (the average number of the sequences with the same Euclidean distance form each generated sequence) [18] show significant effects, especially in a low signal-to-noise ratio (SNR) regime [19–21].

A coded modulation scheme can be modeled as a mapping unit that transforms a sequence of information bits to a sequence of symbols from a multidimensional constellation. Consider k information bits as the input of this unit and its output with n N-dimensional symbols[1]. The design criterion for the optimum N-dimensional constellation in the additive white Gaussian noise (AWGN) channel [8, 10] for high SNR regimes

[1] One may assume a more general case which is a mapping from k bits to an nN-dimensional symbol.

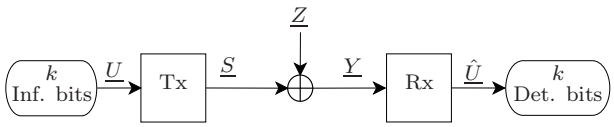

Figure 2.1: An N-dimensional coded data transmission system with k input information bits and k detected bits.

is to maximize the MED for a given average energy of symbols and a given spectral efficiency or a cardinality (number of elements of the set) of the constellation. This problem is well known as sphere packing [22, 23] in mathematics.

Densest sphere packing is defined as an arrangement of non-overlapping identical spheres which fill an N-dimensional space with as large a proportion of the space as possible. The proportion of the space filled by the spheres is called the density of the arrangement [23]. In a lattice arrangement, the centers of the spheres have a regular structure which only needs N vectors (generator matrix) to be uniquely defined (in an N-dimensional Euclidean space). The optimum constellation with large enough cardinality for high SNR regimes [24] is the extracted constellation from an N-dimensional lattice constructed by the densest sphere packing in the N dimensions. The average energy and the cardinality constraints should be fulfilled such that in cutting out this constellation from the original lattice (with an infinite number of signals), the maximum MED is yielded. This optimum constellation gives a nonuniform distribution (probabilistic shaping) for elements of N-dimensional symbols in each dimension [25–27]. The optimum distribution for these elements in terms of achieving capacity is the Gaussian distribution [28], which can be attained as $N \to \infty$. In [29] and [30], some schemes were proposed for 2, 4, 8, 16, and 24 dimensions.

A sub-optimum scheme can be a combination of an independent probabilistic shaping and a coding unit. The probabilistic shaping maps the block of k information bits to nN unequally likely (shaped) symbols. These symbols are selected from a one dimensional pulse amplitude modulation (PAM) constellation. Then, the coding unit encodes these symbols to generate an encoded sequence of symbols with a larger MED. Although some practical systems are built based on this scheme [13], there is no general framework for the design of such a system in the literature.

In this work, the probabilistic shaping is neglected and the analysis is performed solely for a coding unit which receives a block of k information bits and maps them to the n coded N-dimensional symbols. Moreover, because the probabilistic shaping will be ignored, the N-dimensional constellation can be modeled as an N-fold product of one-dimensional constellation with itself [31, 32].

1.1 Equivalent parallel channels

Consider a general coded data transmission system with a block of k input bits $\underline{U}$ in Fig. 2.1. These k bits are mapped to a block of n symbols $\underline{S}$ in the transmitter (Tx). These symbols are selected from an N-dimensional constellation with cardinality 2^{NL}. Then, this symbol block $\underline{S}$ is transmitted through a memoryless AWGN channel, which adds a discrete-time noise vector $\underline{Z}$ with variance $N_0/2$ in each dimension. Finally, the receiver Rx detects a block of k bits $\hat{\underline{U}}$. As was pointed out in Chapter 1, the units Tx and Rx should be determined such that this data transmission system can perform close to the Shannon capacity with affordable complexity.

Before going into the details of these units, we start with a simple case which is

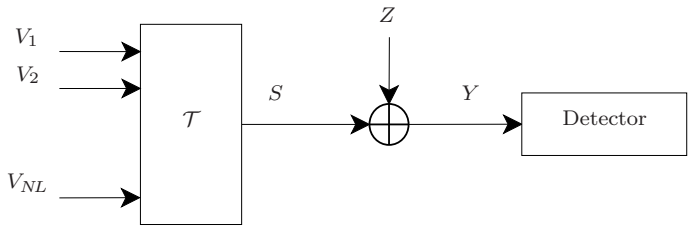

Figure 2.2: An uncoded N-dimensional symbol transmission.

solely an uncoded modulation scheme with $n = 1$ and $k = NL$. As shown in Fig. 2.2, the uncoded scheme receives $k = NL$ bits $V_1,\ V_2,\ \ldots,\ V_{NL}$ and then the mapping unit $\mathcal{T}$ selects an N-dimensional symbol S from the constellation $\mathcal{C}$ with cardinality of 2^{NL}, exploiting these NL bits.

Here we neglect the probabilistic shaping described in the introduction. Therefore, the N-dimensional constellation $\mathcal{C}$ can be assumed as a Cartesian product of N equal one-dimensional constellations $\mathcal{A}$ with cardinality 2^L. This implies that the Tx unit maps k information bits to N selected symbols from a one-dimensional, e.g., PAM constellation $\mathcal{A}$. We call this scheme an N-dimensional coded modulation system in the rest of this report. Here, we exploit the parallel channel approach introduced in [17, 33, 34]. According to Fig. 2.2, the selected symbol S is transmitted through an AWGN channel which adds the discrete noise vector Z with variance $N_0/2$ in each dimension and the channel output is $Y = S + Z$.

The constrained capacity C^{CM} [35], can be written by

$$C^{\mathrm{CM}} \triangleq I(S;Y) = I(V_1,\ldots,V_{NL};Y), \tag{2.1}$$

where $I(S;Y)$ denotes the mutual information between variables S and Y. Using the chain rule [17, 35], this channel can be modeled as NL parallel channels with the inputs $V_i,\ i = 1,\ldots,NL$ and the output Y [17, 33, 34]

$$\begin{aligned} C &= \sum_{i=1}^{NL} I(V_i;Y|V_1,\ldots,V_{i-1}), \\ &\triangleq \sum_{i=1}^{NL} C_i, \end{aligned} \tag{2.2}$$

where $C_i = I(V_i;Y|V_1,\ldots,V_{i-1})$ is the constrained capacity of the parallel channel i provided that the transmitted bits of the channels $1,\ldots,i-1$ are given.

Alternative parallel channels modeling approach is based on using NL parallel, independent decoding of the individual layers (PDL) [17, 34], in which each channel has no information from the input bits of the other channels. The terms parallel channels and layers are used interchangeably in this report. The achievable capacity in this case is $C^{\mathrm{PDL}} = \sum_{i=1}^{NL} I(V_i;Y)$. It can be shown that $I(V_i;Y) \leqslant I(V_i;Y|V_1,\ldots,V_{i-1})$ [17], implying $C^{\mathrm{PDL}} \leqslant C^{\mathrm{CM}}$. The gap between C^{CM} and C^{PDL} strongly depends on the selected labeling of the constellation symbols. Caire *et.al* [34] showed that the gap between C^{CM} and C^{PDL} is surprisingly small with Gray labeling. However, the first scheme (based on (2.2)) is significantly superior to PDL for a finite length code [17].

1.2 Standard coded modulation techniques

We exploit the parallel channel concept to illustrate different coded modulation techniques in the AWGN channels. Consider the unit $\mathcal{T}$, which is a mapping to produce a sequence of symbols from a sequence of input bits. The simplest way to add coding to this uncoded modulation scheme is to encode the information bits by an error-correcting code and then split the encoded stream into segments of length NL bits sequentially. Then each segment is mapped to an N-dimensional symbol. This method, which is the traditional structure of systems with forward error correcting codes, is based on a concatenation of an independent error correcting code and a modulation unit with cardinality 2^{NL}. The method yields suboptimal performance because the previously introduced parallel channels have different constrained capacities for a specific SNR (SNR must not be too high), and it is not considered as coded modulation.

One may instead follow an improved approach by protecting the bits of the channels with lower constrained capacities C_i (bad channels) more than high capacity channels. In other words, in the transmission of coded bits with a single encoder, equally protected bits will experience different channels, i.e. some bits have higher protection than required for the exploited channel and some other bits encounter errors because the code rate [35] is higher than corresponding capacity C_i. Therefore, according to the converse of the channel coding theorem (see Chapter 1), the traditional coded systems are suboptimal. It can be concluded that these parallel channels need unequal error protection. This insight was first used by Ungerboeck [5, 6] in 1976 and then with a different approach by Imai and Hirakawa [7, 36] in 1977. Here, we explain the three main categories of coded modulation schemes[2] exploiting the equivalent parallel channels approach.

Multilevel coded modulation (MLCM)

The basic idea behind MLCM is to exploit an unequal error protecting technique that uses component codes with different rates in layers $1, \ldots, NL$. In contrast to the capacity achieving MLCM scheme [17] based on (2.2), MLCM originally was proposed to maximize the asymptotic minimum Euclidean block distance (MEBD) of the system [7, 36]. Consider that the uncoded MEDs of the constellations for different parallel channels are known for a particular binary labeling (mapping $\mathcal{T}$). Since the MEBD of the scheme depicted in Fig. 2.2 is the minimum MEBD of the layers, the maximum MEBD can be attained by making the MEBD of these layers equal (see Section 3.2). The squared MEBD of each layer is the product of the minimum Hamming distance of the exploited code and the squared uncoded MED of the corresponding layer. Therefore, it was suggested that the Hamming distances of the different layers be assigned such that the MEBD of the layers are equal. MLCM has been shown to be a capacity achieving scheme theoretically [20] and through simulations [17].

An interesting feature of MLCM is the possibility of exploiting a multistage detector according to (2.2) (see Fig. 1.1(b)). The first layer can decode the received block independently from other layers, then the second detector uses the output from the first detector to decode the transmitted bits in this layer. This sequential decoding is followed for the rest of the layers. The multistage decoder has lower complexity than the maximum likelihood (ML) detector. However, it shows a performance degradation in comparison to ML detector.

Trellis coded modulation (TCM)

Ungerboeck [5, 6] introduced a new binary labeling based on the set partitioning technique. The parallel channels resulting from set partitioning have ascending capacity values. The early layers (with smaller indices) have lower capacity values than the layers with indices close NL. The original version of TCM splits the information bits into two

[2] One may assume the continuos phase modulation as a fourth category of this family.

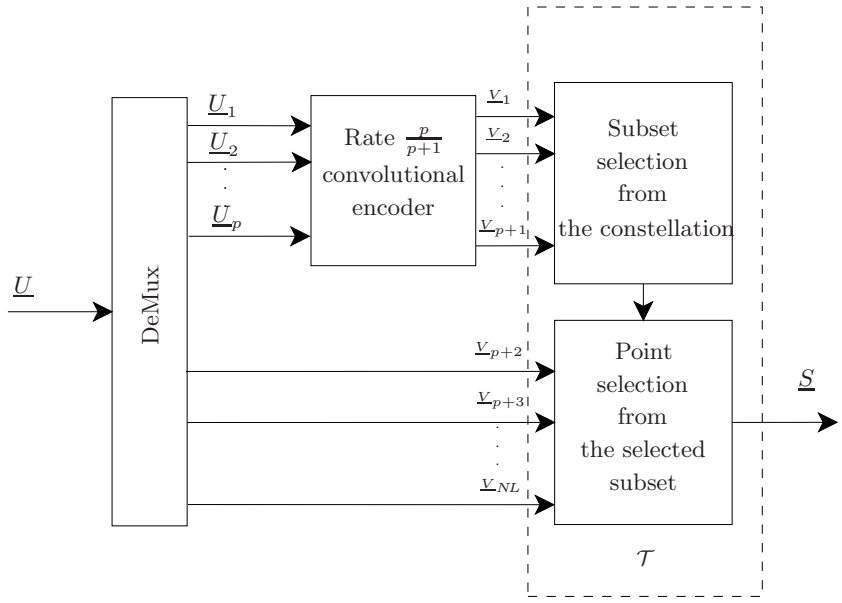

Figure 2.3: TCM block diagram.

groups of layers, where the first group is protected by a convolutional code while the second group remains uncoded (see Fig. 2.3). Although this scheme can be decoded by MSD, Ungerboeck proposed an ML decoder. This decoder first decodes lower layers for all possible bit values of higher layers and then exploits these decisions to do ML decoding of lower layers by the Viterbi [10] algorithm.

Bit-interleaved coded modulation (BICM)

Zehavi [33, 37] proposed the BICM scheme by adding an interleaver between the encoder and the mapping unit $\mathcal{T}$ to distribute the coded bits on different parallel channels uniformly. The block diagram of a BICM scheme is shown in Fig. 2.4. Caire et al. introduced [34] the PDL approach for BICM based on the uniform distribution of encoded bits in different channels. Hence, for sending each encoded bit, a channel is selected among parallel channels uniformly (the probability of using each channel for sending a specific encoded bit is $1/NL$).[3] In other words, the encoded bits at the input of interleaver experience the same channels on average.

BICM was originally proposed to use the channel diversity in order of a bit period. Since different bit positions in a binary labeling experience different channels[4], one may improve the performance of the system by exploiting the diversity in these channels. Interleaving within each labeling bits can yield this diversity. Hence, BICM is superior to TCM and MLCM for fading channels[5] [34, 37]. More detailed information on BICM

[3] Here, we assumed an infinite length interleaver.
[4] Similar to a circumstance that a stream of bits has in a fading channel [37].
[5] Without channel state information at the transmitter.

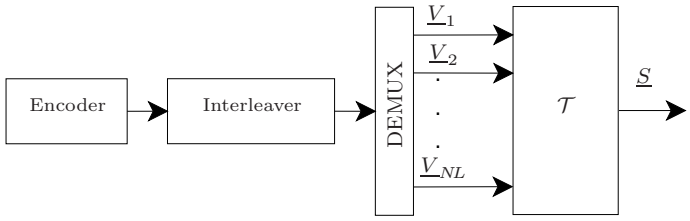

Figure 2.4: BICM block diagram.

can be found in [38, 39].

The suitable coded modulation scheme for fiber-optical channels

In this work, we focus on MLCM rather than the two other main categories of coded modulation techniques, TCM and BICM, for the following reasons:

- A multistage receiver of the MLCM system is an attractive feature for very high speed data transmission links such as fiber-optical channels;
- The MLCM scheme is not as sensitive as the BICM scheme to the hard decision decoding [17] that is commonly used in fiber-optical channels;
- MLCM has not been well investigated for fiber-optical channels.

2 MLCM with multidimensional set partitioning

The MLCM system consists of NL layers (component codes) with the same block length n but different code rates R_i and Hamming distances δ_i for layer i. In the system model shown in Fig. 1.1, the demultiplexing (DEMUX) unit splits the input bit vector $\underline{U}$ of length k bits into NL vectors $\underline{U}_1,\ldots,\underline{U}_{NL}$ of lengths $k_1,\ldots,k_{NL}$, respectively, where $\sum_{l=1}^{NL} k_l = k$. The component codes CC_1, …, CC_{NL} encode these vectors into NL code vectors $\underline{V}_1$, …, $\underline{V}_{NL}$ of length n. An N-dimensional mapper unit $\mathcal{T}$, designed by a set partitioning algorithm, maps NL encoded bits at each time instant to an N-dimensional symbol S.

The channel model is a discrete-time memoryless AWGN channel with noise variance $N_0/2$ in each dimension. A multistage decoder (MSD) with soft or hard decision is applied in the MLCM receiver (see Fig. 1.1). We denote the normalized uncoded MED of the layer i by d_i (normalized with $\sqrt{2\eta E_b}$, where E_b is the average bit energy and η is the spectral efficiency of the system).

In general, an arbitrary labeling of the constellation symbols can define the mapping function $\mathcal{T}$ in Fig. 1.1, but Ungerboeck and block set partitioning [17, 40] provide a simpler receiver structure for the MSD. In this section, we propose a new algorithm for set partitioning of a multidimensional constellation [Paper B] based on the set partitioning of its one-dimensional constituent constellation. It is also shown that the multidimensional constellation has a better trade-off between complexity and performance than one-dimensional constellations [Paper B].

The one-dimensional constellation $\mathcal{A}$ with a normalized MED of d_0 and cardinality of 2^L can be set partitioned into two subsets $\mathcal{A}_0$ and $\mathcal{A}_1$ with normalized uncoded MEDs of

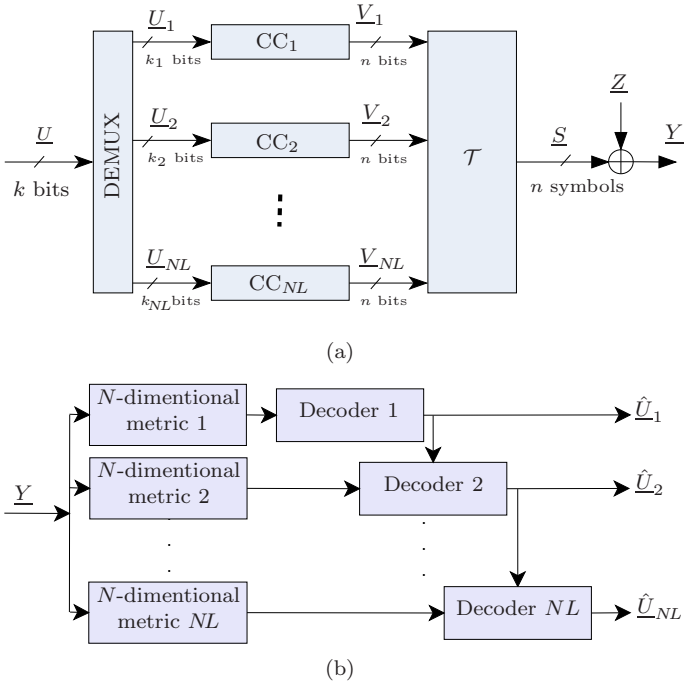

Figure 2.5: (a) An N-dimensional MLCM with NL component codes (layers). (b) Multistage decoder.

$2d_0$. Each of the subsets $\mathcal{A}_0$ and $\mathcal{A}_1$ can be further set partitioned into subsets $\mathcal{A}_{00}$, $\mathcal{A}_{01}$, $\mathcal{A}_{10}$, and $\mathcal{A}_{11}$ and so on, up to L steps with subsets $\mathcal{A}_{x_1,\ldots,x_L}$, $x_i \in \{0,1\}, 0 < i \leq L$ (the same notation as in [17] and [30]). The set partitioning of an N-dimensional constellation $\mathcal{C} = \mathcal{A}^N$, based on the subsets of the one-dimensional constellation $\mathcal{A}$ and the $(N-1)$-dimensional constellation $\mathcal{C}' = \mathcal{A}^{N-1}$, can be written as

$$\begin{aligned}
\mathcal{C}_0 &= \mathcal{A}_0 \times \mathcal{C}'_0 \cup \mathcal{A}_1 \times \mathcal{C}'_1 \\
\mathcal{C}_1 &= \mathcal{A}_0 \times \mathcal{C}'_1 \cup \mathcal{A}_1 \times \mathcal{C}'_0 \\
\mathcal{C}_{00} &= \mathcal{A}_0 \times \mathcal{C}'_0 \ , \ \mathcal{C}_{10} = \mathcal{A}_0 \times \mathcal{C}'_1 \\
\mathcal{C}_{01} &= \mathcal{A}_1 \times \mathcal{C}'_1 \ , \ \mathcal{C}_{11} = \mathcal{A}_1 \times \mathcal{C}'_0 \\
\mathcal{C}_{000} &= \mathcal{A}_{00} \times \mathcal{C}'_{00} \cup \mathcal{A}_{01} \times \mathcal{C}'_{01} \\
\mathcal{C}_{001} &= \mathcal{A}_{00} \times \mathcal{C}'_{01} \cup \mathcal{A}_{01} \times \mathcal{C}'_{00} \\
&\vdots
\end{aligned}$$

assuming that a set partitioning of $\mathcal{C}'$ into $\mathcal{C}'_0$, $\mathcal{C}'_1$, $\mathcal{C}'_{00}$,... is available. For $N = 4$, provided that $\mathcal{A}$ is a PAM constellation labeled by the natural binary code, this method generates Wei's set partitioning [41] approach for four-dimensional QAM. Applying the above recursive approach in NL steps, we can do set partitioning of any N-dimensional constellation $\mathcal{A}^N$.

Example 1: For 16-PAM^2(16-QAM), which is the Cartesian product of two 4-PAM constellations, the set partitioning is done in four steps. In other words, we need four bits to label each symbol from this two-dimensional constellation. If the the first bit of labeling is 0 we proceed with

$$\mathcal{C}_0 = \mathcal{A}_0 \times \mathcal{A}_0 \cup \mathcal{A}_1 \times \mathcal{A}_1,$$

and if this bit is 1, we consider

$$\mathcal{C}_1 = \mathcal{A}_0 \times \mathcal{A}_1 \cup \mathcal{A}_1 \times \mathcal{A}_0.$$

In the next step we assume the first bit was 0 (due to symmetry, one may follow for the first bit equal 1 in a similar way). Now, if the second bit of the labeling is 0, we proceed the mapping into

$$\mathcal{C}_{00} = \mathcal{A}_0 \times \mathcal{A}_0 \ , \ \mathcal{C}_{10} = \mathcal{A}_0 \times \mathcal{A}_1$$

and if it is 1, we move forward to

$$\mathcal{C}_{01} = \mathcal{A}_1 \times \mathcal{A}_1 \ , \ \mathcal{C}_{11} = \mathcal{A}_1 \times \mathcal{A}_0.$$

This procedure is proceeded in L steps to end up with $2L$ ($N = 2$) labeling bits or layers or until one reaches subsets with single point inside them.

Definition: The average number of adjacent symbols of a constellation symbol at the distance of the uncoded MED is the *neighboring coefficient* of the constellation [18, 19] and [Paper A].

The uncoded MED and the neighboring coefficient of each layer are determined by the constellation symbols labeling or the set partitioning method. The neighboring coefficients are used to compute the block error rate of different layers of an MLCM scheme in Section 3.3.

Example 2: Table 2.1 shows the four early steps of this set partitioning for an MLCM scheme with $N = 4$ and 4-PAM as a one-dimensional constituent constellation. The neighboring coefficients of this constellation are 6, 9, $\frac{9}{2}$, $\frac{81}{16}$, 4, 4, 2, 1, and $\frac{1}{10}$, $\frac{2}{10}$, $\frac{2}{10}$, $\frac{4}{10}$, $\frac{4}{10}$, $\frac{8}{10}$, $\frac{8}{10}$, $\frac{16}{10}$ are the squared normalized uncoded MEDs (see Section 2) of layers 1, ..., 8.

Table 2.1: The early four layers of set partitioning of the 256-PAM^4 constellation.

four-dimensional constellation	V_1	subsets	V_2	subsets
$\mathcal{A}\times\mathcal{A}\times\mathcal{A}\times\mathcal{A}$	0	$\mathcal{A}_0\times\mathcal{A}_0\times\mathcal{A}_0\times\mathcal{A}_0$	0	$\mathcal{A}_0\times\mathcal{A}_0\times\mathcal{A}_0\times\mathcal{A}_0$
	0	$\mathcal{A}_1\times\mathcal{A}_1\times\mathcal{A}_1\times\mathcal{A}_1$	0	$\mathcal{A}_1\times\mathcal{A}_1\times\mathcal{A}_1\times\mathcal{A}_1$
	0	$\mathcal{A}_1\times\mathcal{A}_1\times\mathcal{A}_0\times\mathcal{A}_0$	0	$\mathcal{A}_1\times\mathcal{A}_1\times\mathcal{A}_0\times\mathcal{A}_0$
	0	$\mathcal{A}_0\times\mathcal{A}_0\times\mathcal{A}_1\times\mathcal{A}_1$	0	$\mathcal{A}_0\times\mathcal{A}_0\times\mathcal{A}_1\times\mathcal{A}_1$
	0	$\mathcal{A}_0\times\mathcal{A}_1\times\mathcal{A}_1\times\mathcal{A}_0$	1	$\mathcal{A}_0\times\mathcal{A}_1\times\mathcal{A}_1\times\mathcal{A}_0$
	0	$\mathcal{A}_1\times\mathcal{A}_0\times\mathcal{A}_0\times\mathcal{A}_1$	1	$\mathcal{A}_1\times\mathcal{A}_0\times\mathcal{A}_0\times\mathcal{A}_1$
	0	$\mathcal{A}_0\times\mathcal{A}_0\times\mathcal{A}_1\times\mathcal{A}_1$	1	$\mathcal{A}_0\times\mathcal{A}_0\times\mathcal{A}_1\times\mathcal{A}_1$
	0	$\mathcal{A}_1\times\mathcal{A}_1\times\mathcal{A}_0\times\mathcal{A}_0$	1	$\mathcal{A}_1\times\mathcal{A}_1\times\mathcal{A}_0\times\mathcal{A}_0$
	1	$\mathcal{A}_1\times\mathcal{A}_0\times\mathcal{A}_0\times\mathcal{A}_0$	0	$\mathcal{A}_1\times\mathcal{A}_0\times\mathcal{A}_0\times\mathcal{A}_0$
	1	$\mathcal{A}_0\times\mathcal{A}_1\times\mathcal{A}_1\times\mathcal{A}_1$	0	$\mathcal{A}_0\times\mathcal{A}_1\times\mathcal{A}_1\times\mathcal{A}_1$
	1	$\mathcal{A}_0\times\mathcal{A}_1\times\mathcal{A}_0\times\mathcal{A}_0$	0	$\mathcal{A}_0\times\mathcal{A}_1\times\mathcal{A}_0\times\mathcal{A}_0$
	1	$\mathcal{A}_1\times\mathcal{A}_0\times\mathcal{A}_1\times\mathcal{A}_1$	0	$\mathcal{A}_1\times\mathcal{A}_0\times\mathcal{A}_1\times\mathcal{A}_1$
	1	$\mathcal{A}_0\times\mathcal{A}_0\times\mathcal{A}_1\times\mathcal{A}_0$	1	$\mathcal{A}_0\times\mathcal{A}_0\times\mathcal{A}_1\times\mathcal{A}_0$
	1	$\mathcal{A}_1\times\mathcal{A}_1\times\mathcal{A}_0\times\mathcal{A}_1$	1	$\mathcal{A}_1\times\mathcal{A}_1\times\mathcal{A}_0\times\mathcal{A}_1$
	1	$\mathcal{A}_0\times\mathcal{A}_0\times\mathcal{A}_0\times\mathcal{A}_1$	1	$\mathcal{A}_0\times\mathcal{A}_0\times\mathcal{A}_0\times\mathcal{A}_1$
	1	$\mathcal{A}_1\times\mathcal{A}_1\times\mathcal{A}_1\times\mathcal{A}_0$	1	$\mathcal{A}_1\times\mathcal{A}_1\times\mathcal{A}_1\times\mathcal{A}_0$

V_3	subsets	V_4	subsets
0	$\mathcal{A}_0\times\mathcal{A}_0\times\mathcal{A}_0\times\mathcal{A}_0$	0	$\mathcal{A}_0\times\mathcal{A}_0\times\mathcal{A}_0\times\mathcal{A}_0$
0	$\mathcal{A}_1\times\mathcal{A}_1\times\mathcal{A}_1\times\mathcal{A}_1$	1	$\mathcal{A}_1\times\mathcal{A}_1\times\mathcal{A}_1\times\mathcal{A}_1$
1	$\mathcal{A}_1\times\mathcal{A}_1\times\mathcal{A}_0\times\mathcal{A}_0$	0	$\mathcal{A}_1\times\mathcal{A}_1\times\mathcal{A}_0\times\mathcal{A}_0$
1	$\mathcal{A}_0\times\mathcal{A}_0\times\mathcal{A}_1\times\mathcal{A}_1$	1	$\mathcal{A}_0\times\mathcal{A}_0\times\mathcal{A}_1\times\mathcal{A}_1$
0	$\mathcal{A}_0\times\mathcal{A}_1\times\mathcal{A}_1\times\mathcal{A}_0$	0	$\mathcal{A}_0\times\mathcal{A}_1\times\mathcal{A}_1\times\mathcal{A}_0$
0	$\mathcal{A}_1\times\mathcal{A}_0\times\mathcal{A}_0\times\mathcal{A}_1$	1	$\mathcal{A}_1\times\mathcal{A}_0\times\mathcal{A}_0\times\mathcal{A}_1$
1	$\mathcal{A}_0\times\mathcal{A}_0\times\mathcal{A}_1\times\mathcal{A}_1$	0	$\mathcal{A}_0\times\mathcal{A}_0\times\mathcal{A}_1\times\mathcal{A}_1$
1	$\mathcal{A}_1\times\mathcal{A}_1\times\mathcal{A}_0\times\mathcal{A}_0$	1	$\mathcal{A}_1\times\mathcal{A}_1\times\mathcal{A}_0\times\mathcal{A}_0$
0	$\mathcal{A}_1\times\mathcal{A}_0\times\mathcal{A}_0\times\mathcal{A}_0$	0	$\mathcal{A}_1\times\mathcal{A}_0\times\mathcal{A}_0\times\mathcal{A}_0$
0	$\mathcal{A}_0\times\mathcal{A}_1\times\mathcal{A}_1\times\mathcal{A}_1$	1	$\mathcal{A}_0\times\mathcal{A}_1\times\mathcal{A}_1\times\mathcal{A}_1$
1	$\mathcal{A}_0\times\mathcal{A}_1\times\mathcal{A}_0\times\mathcal{A}_0$	0	$\mathcal{A}_0\times\mathcal{A}_1\times\mathcal{A}_0\times\mathcal{A}_0$
1	$\mathcal{A}_1\times\mathcal{A}_0\times\mathcal{A}_1\times\mathcal{A}_1$	1	$\mathcal{A}_1\times\mathcal{A}_0\times\mathcal{A}_1\times\mathcal{A}_1$
0	$\mathcal{A}_0\times\mathcal{A}_0\times\mathcal{A}_1\times\mathcal{A}_0$	0	$\mathcal{A}_0\times\mathcal{A}_0\times\mathcal{A}_1\times\mathcal{A}_0$
0	$\mathcal{A}_1\times\mathcal{A}_1\times\mathcal{A}_0\times\mathcal{A}_1$	1	$\mathcal{A}_1\times\mathcal{A}_1\times\mathcal{A}_0\times\mathcal{A}_1$
1	$\mathcal{A}_0\times\mathcal{A}_0\times\mathcal{A}_0\times\mathcal{A}_1$	0	$\mathcal{A}_0\times\mathcal{A}_0\times\mathcal{A}_0\times\mathcal{A}_1$
1	$\mathcal{A}_1\times\mathcal{A}_1\times\mathcal{A}_1\times\mathcal{A}_0$	1	$\mathcal{A}_1\times\mathcal{A}_1\times\mathcal{A}_1\times\mathcal{A}_0$

3 Rate allocation methods

The most critical part in the design of an MLCM scheme is the analysis of error propagation between the layers. This problem is analyzed by considering ideal interleaver/deinterleaver pairs at each layer [33]. Moreover, Kasami et al. [42, 43] exploited the conditional probabilities of errors, given that the detection of the previous layers was correct. In this section, we introduce a different approach for the rate allocation of an MLCM scheme based on the minimization of the block error rate of the system by considering the error propagation among layers [Paper A].

According to the block diagram in Fig. 1.1, for a specific unit $\mathcal{T}$ (set partitioning), a point to point AWGN channel with multilevel modulation can be modeled with NL equivalent parallel channels. Here, the detector of channel ℓ knows the transmitted bit in the previous channels (layers) $1, \ldots, \ell - 1$. Therefore, the problem is converted into the design of forward error correction units for NL binary channels. However, one should take into account the error propagation from layer ℓ to the layers $\ell + 1, \ldots, NL$ for $\ell = 1, \ldots, NL - 1$ in the rate allocation. This problem is well investigated in the literature as the rate allocation of MLCM component codes.

Many different design rules have been introduced for the design of an MLCM scheme [17, 19, 44]. Here, we continue the design of MLCM scheme by reviewing three efficient algorithms [7, 33] and [Paper A]. The first method is the capacity design rule [17, 33], which is suitable for capacity achieving codes, such as turbo and LDPC codes, while the second and third are useful for less complex codes in high SNR regimes.

3.1 Capacity design rule

According to the chain rule (2.2), the constrained capacity of a point to point channel can be expressed as the sum of the equivalent parallel channels given that the channel ℓ knows the previous transmitted bits $1, \ldots, \ell - 1$. Since our intention is to design the MLCM scheme for a specific coding rate, the total rate is known.

Here, before proceeding further, we use an example to clarify this design rule.

Example 3: Consider the MLCM scheme of *Example* 1 with 16-PAM^2 constellation. Exploiting a numerical approach, the constrained capacity of the overall channel and its equivalent parallel channels for Ungerboeck set partitioning (natural labeling) are shown in Fig. 2.6. If one draws a horizontal line from $C = 3.72$ to cross the channel capacity curve and then by drawing a vertical line from the crossing point to cross the capacity curves of the parallel channels[6], we obtain the capacities $C_1, \ldots, C_4$ of the parallel channels. Through this method, the rates of the capacity achieving component codes can be determined by exploiting the derived capacities, by setting $R_i = C_i$ for $i = 1, \ldots, 4$.

Now, in a general case, the constrained capacity of the original channel C^{CM} and the parallel channels, $C_1, \ldots, C_{NL}$ can be computed by a numerical method. These capacities are determined for a specific binary labeling of a constellation. In the computation of the capacity C_ℓ, it should be taken into account that the early bits $1, \ldots, \ell - 1$ of the binary labeling have been given. Then, using the same approach as *Example* 3, one can readily determine the code rates $R_1 = C_1, \ldots, R_{NL} = C_{NL}$ of the capacity achieving component codes $\mathrm{CC}_1, \ldots, \mathrm{CC}_{NL}$.

3.2 Balanced distance design rule

The minimum MEBD of an MLCM scheme is the minimum MEBD of the MLCM layers. On the hand, the squared MEBD of layer i in an MLCM scheme is $\delta_i d_i^2$ (see Section 2). In order to maximize the MEBD of the MLCM, the MEBD of the different layers should be

[6] As a common redundancy for fiber-optical channels is 7 %, we are especially interested in codes with a total rate $R = 4 \times (1 - 0.07) = 3.72$.

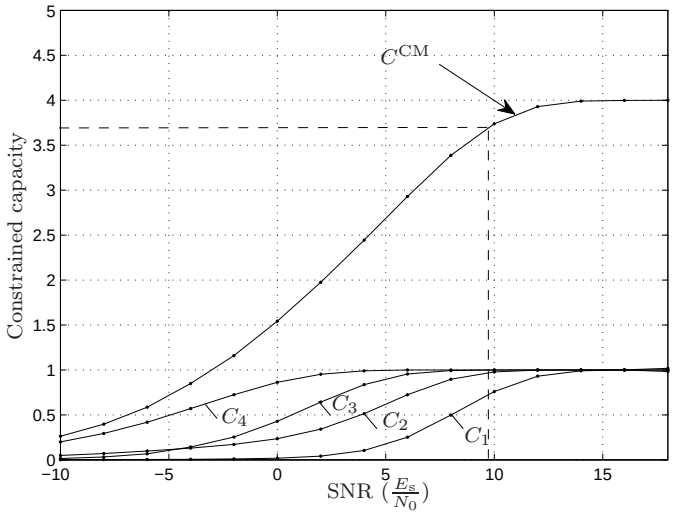

Figure 2.6: Rate allocation with the capacity design rule for different layers of 16-QAM with natural labeling.

equal [17, 33]. Therefore, the rate allocation of MLCM layers can be accomplished such that it supports the same MEBD for each layer. This goal can be attained by choosing Hamming distances of different layers such that the MEBD of layers are balanced, i.e. The larger Hamming distance for smaller uncoded MED and vice versa. Since we neglect the effect of neighboring coefficient, this design criterion is optimum for high SNR regimes.

3.3 Lagrange multiplier method

We introduce a new rate allocation method based on the minimization of the total block error rate (BLER) of the system using the Lagrange multiplier approach [Paper A]. Since this design approach exploits the union bound [9] to compute the BLER of each layer, it is suitable for reasonably high SNR regimes. The idea behind this method is very simple. The total BLER of an MLCM scheme can be written using union bound. Due to the existence of a combinatorial function inside the expression of BLER, in general, it is considered to be a non-convex function of the exploited code rate. We exploit a second order polynomial approximation [Paper A] to make it convex. Then the minimization is done based on the Lagrange multiplier approach. The constraint of this optimization problem is the total code rate of the system. In the computation of BLER of each layer, we need the uncoded bit error rate of each layer. This bit error rate P_{b} can be computed by

$$P_{\mathrm{b}} \approx N_i Q(\frac{d_i}{\sqrt{2N_0}}),$$

where N_i and d_i denote the neighboring coefficient and the uncoded MED of layer i.

Example 4: Fig. 2.7 shows the rate allocation of an MLCM scheme with a 16-QAM constellation; the total code rate of 3.28, and the Ungerboeck's set partitioning as the mapping unit $\mathcal{T}$. As seen in this figure, the optimum rate allocation is a function of

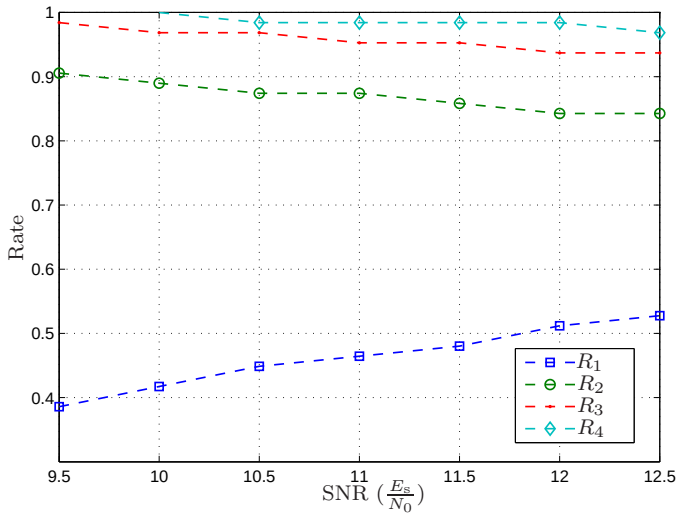

Figure 2.7: Rate allocation of 16-QAM layers with Lagrange multiplier method, total rate = 3.28.

SNR. In high SNRs the result of this method tends to the balanced distance rule while in moderate SNRs the resulted rate allocation is very close to capacity design rule. In moderate and low SNRs, both neighboring coefficients and uncoded MED are important in rate allocation whereas in high SNRs, the uncoded MED plays the main role.

Chapter 3

Fiber-optical channels

An optical fiber is a cylindrical dielectric waveguide (nonconducting waveguide) consisting of a core surrounded by a cladding layer. Light propagates along the axis of this channel by internal reflection. The optical signal will travel in the core because its refractive index is greater than that of the cladding. Transverse modes exist because of boundary conditions imposed on the light by the fiber [45, ch. 3]. The allowed modes can be determined by solving Maxwell's equations for the boundary conditions of a given fiber [46, ch. 2]. Fibers with more than one mode are called multi-mode optical fibers. These types of fibers are usually used in noncoherent data transmission for short range (distance) links. In contrast, the single-mode optical fibers (SMF) are mostly exploited in coherent and long-haul communication systems.

Light is modulated as an electromagnetic signal to convey information bits in fiber-optical channel. In this chapter, to investigate channel models for a single-mode fiber link, we start with a general model in Section 1 and then in Section 2, a simplified model corresponding to a practical scenario is derived. Section 3 describes the statistics of the received signal in dispersion-managed links for a single-polarization. Finally, the optimum detector for a data transmission system in this channel is introduced in Section 4.

1 General channel model

The propagation of a linearly polarized electric field $E(z,t)$ over an optical fiber is described by the standard nonlinear Schrödinger equation (NLSE) [46]

$$j\frac{\partial E}{\partial z} + \gamma|E|^2E + j\frac{\alpha}{2}E = \frac{\beta_2}{2}\frac{\partial^2 E}{\partial t^2}, \tag{3.1}$$

where z is the propagation distance and t is time. Here, we assume $E_0 = E(0,t)$ is the baseband envelope of a single-polarized signal launched into a fiber channel with a Kerr nonlinear parameter γ, an attenuation factor α, and a group delay β_2. According to the NLSE [47, 48] excluding the fiber attenuation factor, fiber impairments are in principle two phase effects: the chromatic dispersion [49, 50], which causes a phase multiplication in the frequency domain with no change in the amplitude of the spectrum (the NLSE term with factor β_2), and the Kerr effect [51, 52], which shows no change in the amplitude but a phase multiplication in the time domain (the NLSE term with factor γ). In principle, chromatic dispersion can be modeled as an all-pass filter that can introduce memory into the channel.

The order of these two phase effects is determined by exploiting the insight that nonlinear effects are most significant at the beginning of a fiber span where the signal

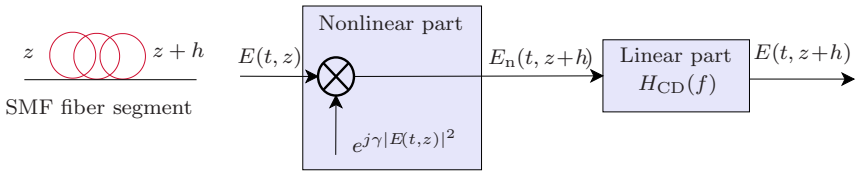

Figure 3.1: A model of an SMF fiber segment as a concatenation of the linear and nonlinear part.

has the highest power [47]. Therefore, the Kerr-effect rotates the phase of transmitted signal first, before linear propagation. This heuristic helps us to model a reasonably short fiber segment with length h as a concatenation of nonlinear (Kerr effect) and linear (chromatic dispersion) blocks, as shown in Fig. 3.1.

Due to the fiber attenuation α, optical amplifiers must be inserted periodically, typically every 50–100 km in a long-haul fiber link. We call each period a span of the fiber link. Usually, each span consists of an SMF fiber, a DCF fiber (to compensate the dispersion effect of the SMF fiber), and an amplifier. The length of the mentioned short segment h for different scenarios can be assumed smaller, equivalent, or greater than the length of a span in a fiber link. Generally, there are two types of amplifiers for a fiber link: discrete (lumped) and distributed amplifiers [46, ch. 8 and 9].

We proceed the system model by assuming a fiber link with total length L and N spans of discrete (lumped) amplifiers, where the fiber loss is compensated perfectly. Each amplifier adds complex circularly symmetric Gaussian amplified spontaneous emission (ASE) noise n_k, $k = 1, \ldots, N$ in each polarization with variance σ_0^2. Moreover, we consider the noise within an optical signal bandwidth, ignoring the Kerr effect induced from out-of-band signal and noise similarly as [53] and assume the system uses a nonreturn-to-zero (NRZ) pulse shape. A good approximate channel model [47] based on the NLSE and the above considerations is shown in Fig. 3.2. In this model, a dispersion compensation fiber (DCF) is included in each fiber span to mitigate the dispersion effect of the SMF fiber.

Here, we assumed $h = L/(2N)$ as a length of the SMF and DCF fibers in each span. Although based on this model the propagation of a signal in the fiber link is illustrated simply by a concatenation of a linear and a nonlinear block, the derivation of the statistics of the received signal based on this model is still cumbersome. Therefore, we neglect the effect of chromatic dispersion in the rest of this report. This makes the analysis applicable to dispersion-managed systems, similarly as was done in [53, 54], for example.

2 Dispersion-managed fiber links

In this section, we describe the system model for a fiber channel without memory (dispersion). We begin the investigation of the system model for discrete amplification and then we extend it for a distributed case.

By neglecting chromatic dispersion ($\beta_2 = 0$), the solution to (3.1) for a single span of length $\frac{L}{N}$ can be written by

$$E(\frac{L}{N}, t) = E_0 \exp\left(j\gamma L_{\mathrm{eff}}|E_0|^2 - \frac{\alpha L}{2N}\right), \tag{3.2}$$

where $L_{\mathrm{eff}} = (1 - e^{-\alpha L/N})/\alpha$ is the effective length of each fiber span. Here, we considered $\gamma = \gamma_{\mathrm{SMF}} = \gamma_{\mathrm{DCF}}$. The simplified model for this case is shown in Fig. 3.3.

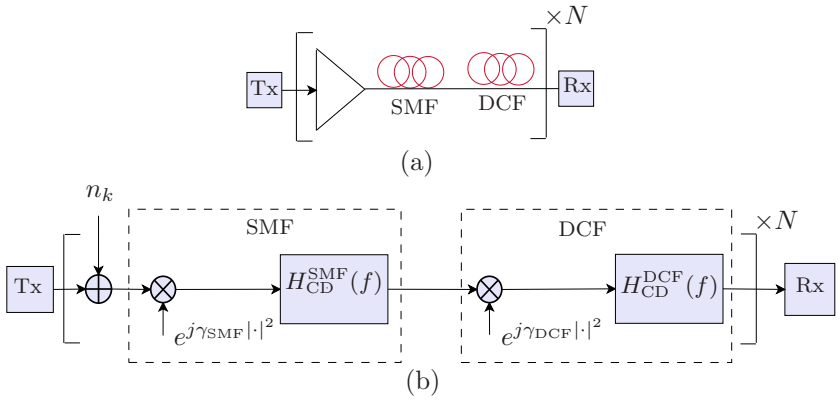

Figure 3.2: (a) A fiber link with N spans where each one consists of an amplifier, an SMF fiber, and a DCF fiber. (b) An approximate model of (a).

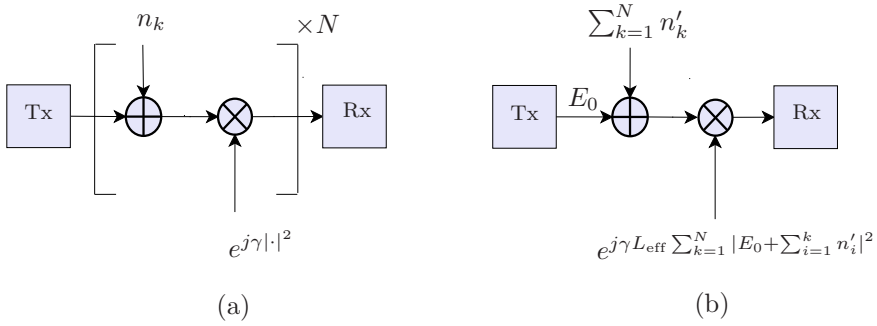

Figure 3.3: (a) A dispersion-managed fiber link with N spans which each one consists of an amplifier, an SMF fiber, and a DCF fiber. (b) An equivalent model for (a). (n'_k is the circularly rotated version of n_k with a random phase value)

The received electric field can be written by [53, 55, 56]

$$E = \hat{E} e^{j\phi_{\mathrm{n}}}, \tag{3.3}$$

where $\hat{E} = E_0 + \sum_{k=1}^{N} n'_k$; the term ϕ_{n} is generated by interaction of the signal and noise

due to the Kerr effect, as

$$\phi_{\rm n} = \gamma L_{\rm eff} \sum_{k=1}^{N} |E_0 + \sum_{i=1}^{k} n_i'|^2, \tag{3.4}$$

and the noise n_k' is given by

$$n_k' = n_k \exp\left(-j \sum_{p=1}^{k-1} |E_0 + \sum_{i=1}^{p} n_i'|^2 \right).$$

Since $\sum_{p=1}^{k-1} |E_0 + \sum_{i=1}^{p} n_i'|^2$ is independent of n_k, it is readily seen that n_k' has a circular Gaussian distribution with the same variance and mean value as n_k. Therefore, we can drop the primes and proceed the analysis with n_k instead of n_k'. The phase trem $\phi_{\rm n}$ in (3.4) is known as nonlinear phase noise and it is generally believed to be a major impairment in long-haul optical transmission system [51–53].

By definition, $E = E(L/N, t)$ is a time dependent electric field, not a vector representation of the projected received electric field in a signal space. We nevertheless use (3.3) to model the discrete-time system, where E is a complex signal vector. This is a standard approximation in the field and has been shown numerically [57, 58] to be reasonably accurate, although the theoretical justification is insufficient.

One may consider the distributed amplification as a discrete lumped amplification with infinite number of spans. This gives $\lim_{N\to\infty} NL_{\rm eff} = L$. In this case, a continuous amplifier noise $n(z)$ is considered as a zero mean complex-valued Wiener process with autocorrelation function of [59, p. 154]

$$\mathrm{E}[n(z_1)n^*(z_2)] = \sigma_{\rm d}^2 \min(z_1, z_2),$$

where $\sigma_{\rm d}^2 = N\sigma_0^2/L$. The nonlinear phase noise can be computed for distributed amplification by

$$\phi_{\rm n} = \frac{\gamma N L_{\rm eff}}{L} \int_0^L |E_0 + n(z)|^2 \mathrm{d}z. \tag{3.5}$$

The ASE noise $n(L)$ generated by in-line amplifiers in two polarizations and accumulated at the receiver has the variance $L\sigma_{\rm d}^2 = 2h\nu_{\rm opt} W L \alpha n_{\rm sp}$ [60], where $h\nu_{\rm opt}$ is the energy of a photon, $n_{\rm sp}$ is the spontaneous emission factor, and W is the bandwidth of the optical signal. The SNR ρ is defined as $|E_0|^2/(L\sigma_{\rm d}^2)$ and $|E_0|^2/(N\sigma_0^2)$ for distributed and lumped amplification, respectively.

3 Statistics of a single-polarization signal

In general, the derivation of signal statistics is inevitable for design of a maximum likelihood receiver for a data transmission system. As we pointed out, the statistics of the received signal for a fiber channel described by the standard NLSE is unknown in the literature. In this section, we describe the derivation of the statistics of a received signal for a dispersion managed fiber studied in [59, ch. 5] [54–56, 61–65], which is based on the system model of Section 2.

First, we describe the probability density function (pdf) of nonlinear phase noise in Section 3.1, and the joint pdf of the amplitude and phase of the received signal for this channel is investigated in Section 3.2. This section helps the reader follow the results in [Paper D], and thus we have tried to keep all the notations consistent.

3.1 Nonlinear phase noise

In this section, due to the computational difficulty of the pdfs, we first compute the characteristic functions. Then we compute the pdf by taking the inverse Fourier transform of its characteristic function [66]. The analysis is done for distributed and lumped amplification separately.

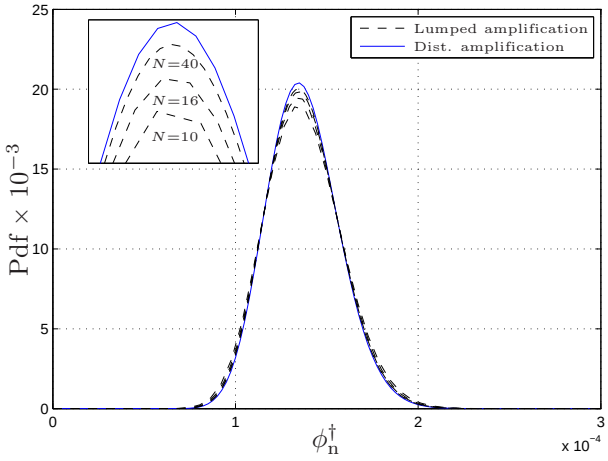

Figure 3.4: Pdfs of the normalized nonlinear phase noise for a fiber link with distributed ($\phi_{\mathrm{n}}^{\dagger} = \phi_{\mathrm{n}}/L$) and lumped ($\phi_{\mathrm{n}}^{\dagger} = \phi_{\mathrm{n}}/(NL_{\mathrm{eff}}$; $N = 10,\ 16,$ and 40) amplification ($L = 4000$ km, $\gamma = 1.2$ (W km)$^{-1}$, $\alpha = 0.25$ dB/km, SNR = 15 dB, and 42.7 Gbaud).

Distributed amplification

For distributed amplification, the characteristic function of ϕ_{n} is given[1] in [59, p. 157] by

$$\Psi_{\Phi_{\mathrm{n}}}(\nu) = \sec\left(L\sigma_{\mathrm{d}}\sqrt{j\gamma\nu}\right)\exp\left(\rho L\sigma_{\mathrm{d}}\sqrt{j\gamma\nu}\ \tan\left(L\sigma_{\mathrm{d}}\sqrt{j\gamma\nu}\right)\right). \tag{3.6}$$

The pdf of the nonlinear phase noise can be computed by taking the inverse Fourier transform from this characteristic function. Figure 3.4 shows this pdf for two different SNRs, 10 and 20 dB.

Lumped amplification

The characteristic function of the nonlinear phase noise for a single-polarization system with lumped amplification has been derived in [59, ch. 5] as

$$\Psi_{\Phi_{\mathrm{n}}}(\nu) = \prod_{k=1}^{N}\frac{1}{1 - j\gamma L_{\mathrm{eff}}\nu\lambda_k\sigma_0^2}\exp\left(\frac{j\gamma\nu E_0^2 L_{\mathrm{eff}}(\mathbf{\Lambda}_k\boldsymbol{\chi})^2}{\lambda_k - j\gamma L_{\mathrm{eff}}\nu\lambda_k^2\sigma_0^2}\right), \tag{3.7}$$

where $\boldsymbol{\chi} = (N, N-1, \ldots, 2, 1)^{\mathrm{T}}$, and λ_k and $\mathbf{\Lambda}_k$ are the eigenvalues and eigenvectors, respectively, of the covariance matrix [59, p. 149]

$$\mathbf{\Pi} = \begin{pmatrix} N & N-1 & N-2 & \ldots & 1 \\ N-1 & N-1 & N-2 & \ldots & 1 \\ \vdots & \vdots & \vdots & \ddots & \vdots \\ 1 & 1 & 1 & \ldots & 1 \end{pmatrix}.$$

[1] The nonlinear phase noise ϕ_{n} in [59, p. 157] was normalized by $\gamma L^2\sigma_{\mathrm{d}}^2$.

The plot of this pdf is shown in Fig. 3.4 for 10, 16, and 40 spans. As seen in this figure, the pdf for $N > 32$ spans is almost overlapped with its corresponding distributed system.

3.2 The joint pdf of the amplitude and phase of the received signal

In this section, the statistics of a single-polarization signal after propagation through a fiber channel are described for distributed and lumped amplifications. The normalized received amplitude r is defined as $|E_0|/(\sigma_{\rm d}\sqrt{L})$ and $|E_0|/(\sigma_0\sqrt{N})$ for distributed and lumped amplifications, respectively. The joint pdf of the received phase θ and the normalized amplitude r of a dispersion-managed fiber channel with *distributed amplification* is [59, p. 225]

$$f_{\Theta,R}(\theta,r) = \frac{f_R(r)}{2\pi} + \frac{1}{\pi}\sum_{k=1}^{\infty} \mathrm{Re}\left\{C_k(r)e^{jk(\theta-\theta_0)}\right\}, \tag{3.8}$$

where $f_R(r) = 2re^{-(r^2+\rho)}I_0(2r\sqrt{\rho})$ is the pdf of the Ricean random variable r and θ_0 is the initial transmitted phase. Moreover, the Fourier series coefficients are

$$C_k(r) = \frac{r\Psi_{\Phi_{\rm n}}(k)}{\tau^2(k)} \exp\left(-\frac{r^2+|m(k)|^2}{2\tau^2(k)}\right) I_k\left(\frac{m(k)r}{\tau^2(k)}\right), \tag{3.9}$$

where k is a positive integer, $\tau^2(\nu) = \frac{\tan(L\sigma_{\rm d}\sqrt{j\gamma\nu})}{2L\sigma_{\rm d}\sqrt{j\gamma\nu}}$, $m(\nu) = \sqrt{\rho}\sec(L\sigma_{\rm d}\sqrt{j\gamma\nu})$, $I_q(\cdot)$ denotes the $q^{\rm th}$-order modified Bessel function of the first kind, and $\Psi_{\Phi_{\rm n}}(j\nu)$ is given in (3.6).

In the case of *lumped amplification*, the joint pdf of the received phase θ and the normalized amplitude r of a dispersion-managed fiber channel can be derived as (3.8), where $\Psi_{\Phi_{\rm n}}(j\nu)$ is given in (3.7),

$$\tau^2(\nu) = \sigma_0^2 \sum_{k=1}^{N} \frac{(\mathbf{\Lambda}_k.\boldsymbol{\chi})^2}{1-j\gamma\nu L_{\rm eff}\lambda_k\sigma_0^2},$$

$$m(\nu) = E_0 \sum_{k=1}^{N} \frac{(\mathbf{\Lambda}_k.\boldsymbol{\chi})(\mathbf{\Lambda}_k.\mathbf{\Gamma})/\lambda_k}{1-j\gamma\nu L_{\rm eff}\lambda_k\sigma_0^2},$$

in which $\mathbf{\Gamma} = (1,1,\ldots,1)^{\rm T}$, $\cdot$ is the inner product of the two vectors, and the rest of the parameters are the same as introduced in the distributed case. Figure 3.5(a) shows the joint pdf of the amplitude and phase of the received signal for a 16-point constellation with the transmitted power of 0 dBm and the following channel parameters: $L = 5000$ km, $\gamma = 1.2$ (W km)$^{-1}$, $\alpha = 0.25$ dB/km, and 42.7 Gbaud.

3.3 Application of signal statistics

The described statistics in Section 3.2 are needed in the design of an optimum receiver based on minimum mean square error or maximum likelihood. In other words, pre and postcompesation of nonlinear phase noise (see Section 4) should be done such that the performance of the system is optimized. In order to minimize the error probability of the system, the suitable compensation can be derived by exploiting the statistics of the received signal. Moreover, the design of a coded scheme for such a system can be accomplished provided that the statistics of the signal after postcompensation are known. The design of multilevel coded modulation scheme based on the derived statistics in this chapter is introduced in [Paper C]. Furthermore, statistics of received signals for a data transmission system with dual-polarization in a dispersion managed fiber, for the first time, are derived in [Paper D]. One may design an ML detector by exploiting the results of [Paper D].

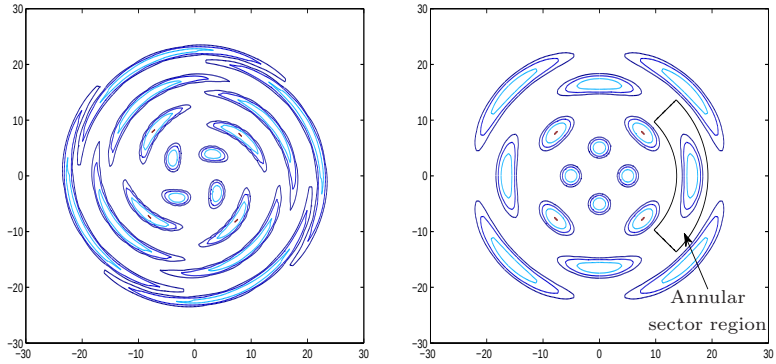

(a) (b)

Figure 3.5: The joint pdf of the amplitude and phase of (a) the received signal, (b) the complex signal $re^{j\theta'}$, for a 16-point constellation (see Section 4.1). Values of contours are $10^{-2.5}, 10^{-2}, \ldots, 1$. The transmitted constellation has been plotted in Fig. 4.2(a).

4 Nonlinear phase noise compensation

The correlation of the received amplitude and the nonlinear phase noise can be exploited to compensate the nonlinear phase noise from the received phase at the receiver in a single step [60, 67–69]. However, some approaches have been proposed to mitigate the effect of nonlinear phase noise by predistortion [69–71] at the transmitter. Since the statistics of the received signal is not known analytically for a channel with both chromatic dispersion and nonlinear phase noise, a back-propagation approach [47] based on the approximate model in Fig. 3.2 must be used. In that case, the signal is passed through a fiber with a negative nonlinearity and chromatic dispersion to compensate for nonlinear phase noise and chromatic dispersion jointly. Since negative nonlinearity is not easily available, this is performed numerically using the split-step Fourier methods [70, 72, 73]. In contrast, as we described Section 3, due to the availability of the statistics of dispersion managed links, the design of an optimal detector is possible for this case.

The optimal detector should minimize the error probability of the system after compensation of nonlinear phase noise. Hence, the maximum a posteriori probability (MAP) detector is optimum in terms of minimizing the error probability of the system. But since the derivation of optimal detector is analytically complicated, two detectors were proposed based on linear [67] and minimum mean square error [59, ch. 6] compensation of nonlinear phase noise. The linear compensator was optimized in terms of the variance of the residual nonlinear phase noise. In parallel to theoretical methods, some experimental schemes were demonstrated based on this linear minimum mean square error [68] and other empirical methods [74].

In this section, we describe the optimal maximum a posteriori probability detector for compensating nonlinear phase noise. The derived pdf of the nonlinear phase noise and the joint pdf of the amplitude and phase of the received signal can be exploited to show that the received amplitude is solely needed to estimate the added nonlinear phase

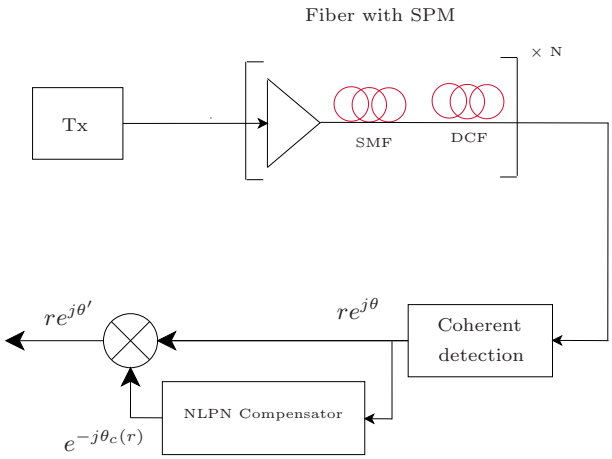

Figure 3.6: The system model with the optimal MAP nonlinear phase noise (NLPN) compensator.

noise in the channel. This optimal MAP detector is superior to the detector based on the linear compensator proposed in [75] in terms of performance (at the expense of higher complexity) and slightly better than the minimum mean square scheme of [59, ch. 5] with nearly the same complexity.

4.1 The MAP detector

The optimal MAP receiver can be derived exactly for an M-PSK signal set in which the phases of the signal alternatives are $\theta_k = \frac{(2k-1)\pi}{M}$, $k = 1, \ldots, M$. One can readily derive the ML decision boundary [9] between the symbols with the phases θ_1 and θ_M, exploiting the joint pdf of the amplitude and phase of the received signal given that the transmitted symbol is one of these two symbols. It was shown in [60] that the ML decision boundaries are rotated by

$$\theta_c(r) = \angle\, C_1(r), \tag{3.10}$$

where $\angle$ denotes the phase of a complex number. This rotation is a nonlinear (second order polynomial) function of the received signal amplitude r for a fiber channel with a distributed amplification.

By symmetry, the decision boundaries between phases θ_k and θ_{k+1}, for $k = 1, \ldots, M$ are obtained as $\theta_c(r) + \frac{2k\pi}{M}$, where θ_{M+1} is equivalent to θ_1. Moreover, as shown in Fig. 3.6, we can derotate the decision boundaries between symbols to get almost straight line decision boundaries. This approach makes the receiver very simple to implement. In brief, the nonlinear phase noise compensator computes the phase rotation of decision boundaries based on the received amplitude. This rotation is canceled out by multiplying the received signal $re^{j\theta}$ with $e^{j\theta_c}$ as shown in Fig. 3.6.

By using (3.10) and (3.8), the joint pdf of the amplitude and phase of the signal

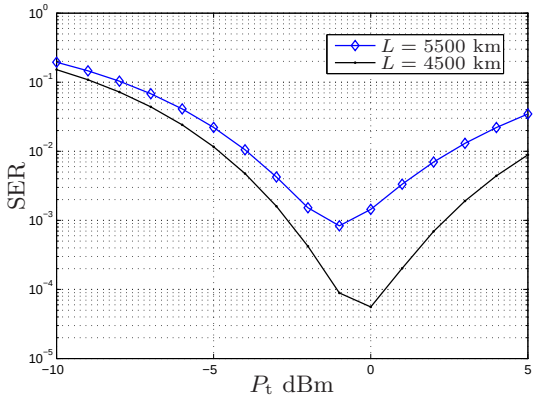

Figure 3.7: The SER of a dispersion-managed fiber link with $L = 4500$ and 5500 km.

$re^{j\theta'} = re^{j(\theta-\theta_c(r))}$ (after the nonlinear compensator, see Fig. 3.6) is obtained by

$$f_{R,\Theta'}(r,\theta') = \frac{f_R(r)}{2\pi} + \frac{1}{\pi}\sum_{k=1}^{\infty}|C_k(r)|\cos\left(k\left(\theta'-\theta_0\right)\right), \tag{3.11}$$

where f_R and C_k were defined in Section 3.2.

Figure 3.5(b) shows the joint pdf of the amplitude and phase of the received signal after nonlinear phase noise compensation ($re^{j\theta'}$) for a 16-point constellation with the transmitted power of 0 dBm and the following channel parameters: $L = 5000$ km, $\gamma = 1.2$ (W km)$^{-1}$, $\alpha = 0.25$ dB/km, and 42.7 Gbaud. As seen in Fig. 3.5(b), the decision boundaries are either straight lines or circular arcs and the annular sector region (a sector in the area between the two concentric circles) can be used to perform the detection in two steps. The symbol error rates (SER) for this system with the following radii of the rings[2]: $R_1 = 0.28\sqrt{P_t}, R_2 = 0.66\sqrt{P_t}, R_3 = 1.06\sqrt{P_t}, R_4 = 1.53\sqrt{P_t}$ are shown in Fig. 3.7 for $L = 4500$ and 5500 km. In high SNR regimes ($P_t > 0$ dBm), unlike AWGN channels, the SER increases. This behavior is due to nonlinear phase noise effect, which shows major degradation in high transmitted powers.

[2]This radii distribution is selected by performing a numerical optimization to minimize the SER for transmitted power $P_t = -4$ dBm

Chapter 4

Coded modulation for fiber-optical channels

Traditional error correcting codes such as Bose–Chaudhuri-Hocquenghem (BCH), Reed–Solomon, Reed–Muller, and others, are designed for binary-input AWGN channels. The criterion for the design of these codes is the maximization of the minimum Hamming distance of generated code words. These classic codes were designed based on a geometrical approach (increasing the minimum distance between codeword pairs), while the capacity achieving codes such as turbo codes [76–80], low density parity check codes [81], and polar codes [82] were originally proposed by inspiration from information theory [83]. The capacity achieving codes were optimized for binary-input AWGN, binary symmetric (BSC) and binary erasure (BEC) channels.

The coding theory for non-Gaussian channels, especially fiber-optical channels, is not well investigated. The lack of an accurate statistical model for a general fiber-optical channel (described by NLSE) might be the main reason for the absence of analytical results in the design of error correcting codes for these channels. Recently, many new approaches based on the capacity achieving codes [84] have been proposed for new optical data transmission systems. These schemes intend to increase the performance of the system in moderate SNR regimes where the classic Reed–Solomon codes show poor performance [3, 85, 86].

Significant efforts have been devoted to evaluating the performance of existing codes in the literature [78, 79]. Since the core of coded modulation techniques is an error correction component code, selected from the classic [10] or capacity achieving codes [10, 81], these binary codes need to be adapted to perform optimally in fiber channels. Interestingly, it has been claimed that LDPC code designed for AWGN channels can perform close to optimal in non-Gaussian channel as well [87].

In [84], the performance of two different classes of capacity achieving codes were evaluated in optical systems. It was shown that LDPC codes are in general more suitable than turbo product codes because they are more robust to the effect of quantization on the log-likelihood ratio.

Here we will leave the design of optimum binary error correcting codes of fiber-optical channels, and proceed with coded modulation techniques optimized for these channels. Recently, some coded modulation techniques based on BICM [88, 89], TCM [77, 90], and MLCM [89] have been proposed for fiber-optic channels. In all of those works, the design criteria of the proposed methods are the same as for typical AWGN channels.

In this chapter, for the first time [Paper C], we introduce a different design criterion in

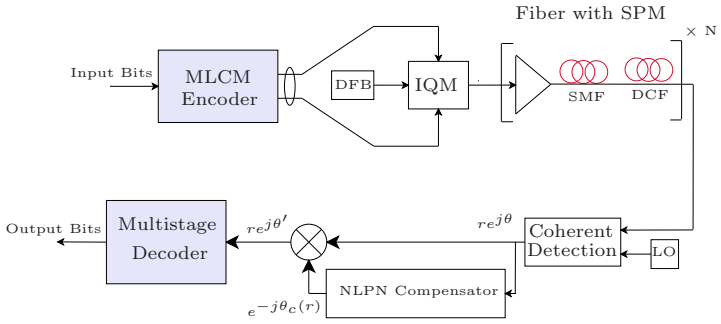

Figure 4.1: The system model with the optimal MAP nonlinear phase noise (NLPN) compensator.

the design of coded modulation techniques for dispersion-managed fiber-optical channels. The new method exploits the statistics of complex received signal for this channel and minimizes the total block error rate of the system. In the following, we first describe the system model and then the MLCM scheme for these channels.

1 System model

In this section, we assume the nonlinear phase noise has been compensated by the MAP algorithm proposed in Section 4. Therefore, the exploited coded modulation technique protects the symbols against the ASE noise and residual nonlinear phase noise. The joint pdf of the received amplitude and phase is given in (3.11). Here we assume that the initial transmitted phase is θ_0. The block diagram of an optical communication system with an MLCM encoder and an MSD is shown in Fig. 4.1. According to the proposed block diagram of Fig. 4.1, the MLCM unit produces a complex I/Q symbol and the optical I/Q modulator (IQM) transforms the generated complex symbol to an I/Q modulated signal.

2 Rate allocation of MLCM scheme in dispersion-managed fiber channels

In general, a rate allocation is performed for a particular mapping unit $\mathcal{T}$ (see Fig. 1.1). In general, an ML detector for quadrature amplitude modulation is not a practical scheme for dispersion-managed fiber channels. This is due to the non-symmetric decision regions of constellation symbols. Instead of an exact ML detector, a two stage detector is proposed in [60], which has a performance close to an ML detector but has very low complexity (see Section 4). In this detector, first the amplitude of the received signal is detected and then in the second stage, the phase of the received signal is determined based on the detected amplitude in first step. It is shown [60] that a ring constellation consisting of many M-PSK constellations with different amplitudes shows better performance than a square QAM constellation with the same number of symbols. A heuristic choice of mapping $\mathcal{T}$ is to start by choosing a ring and then a phase for the symbol inside the selected ring of the constellation. Here, we proceed the design by introducing an example.

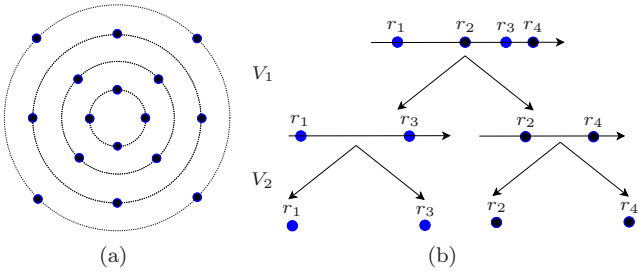

Figure 4.2: (a) 16-point ring constellation. (b) Radius set partitioning of the ring constellation.

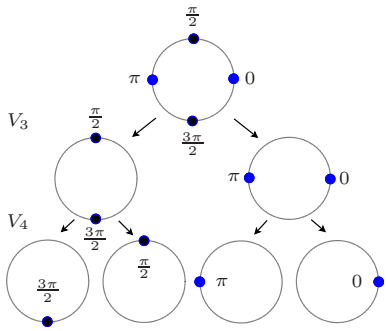

Figure 4.3: Phase set partitioning of the ring constellation.

Example 5: Consider a 16-point ring constellation with four rings with four equally spaced phase symbols in each ring (see Fig. 1.4(a)). As seen in Fig. 1.4(b), the first two bits determine the set partitioning of amplitude and the last two bits of binary labeling (see Fig. 1.5) control the set partitioning of symbols inside each ring. The radii of the ring constellation are selected by a numerical search method as $(0.28, 0.66, 1.06, 1.53)\sqrt{P_t}$ to reach the minimum SER for uncoded data transmission in the nonlinear regime (high transmit power). However, this approach can be applied for an arbitrary radii distribution.

2.1 Capacity design rule

We have defined the set partitioning approach, now we need to determine the component code rates. One may use the capacity design rule to allocate the code rates of different

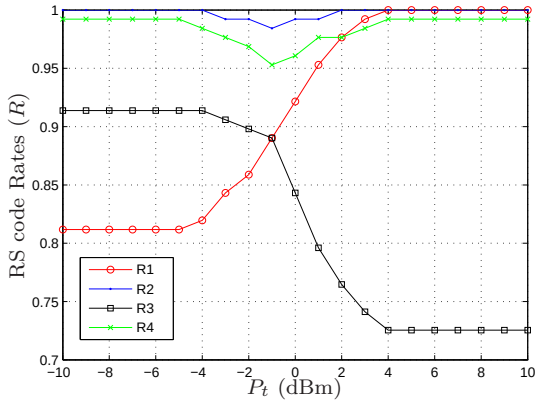

Figure 4.4: Optimum rate allocation of MLCM RS component codes for $L = 5000$ km.

layers. We therefore need to compute the constrained capacity of the MLCM layers as

$$\begin{aligned} C_1 &= I(V_1; r) \\ C_2 &= I(V_2; r|V_1) \\ C_3 &= I(V_3; \theta'|r) \\ C_4 &= I(V_4; \theta'|V_3, r). \end{aligned} \tag{4.1}$$

Once these capacities are computed, the rate of LDPC codes can be selected for different layers corresponding to computed constraint capacities (see Section 3.1). We leave exploiting capacity achieving codes for future work and continue the design using Reed–Solomon codes. Since these codes are not capacity achieving codes, we use the Lagrange multiplier approach, which is an optimum method for reasonably high SNR regimes (see Section 3.3).

2.2 Lagrange multiplier method

For a fixed constellation and a fixed mapping $\mathcal{T}$, the major difference between the design of an MLCM scheme for an AWGN channel and an optical nonlinear channel is in the uncoded bit error rate of different layers. We included the details of the computation of these uncoded bit error rates in [Paper C]. One may readily exploit the Lagrange multiplier method [Paper A] to compute the rates of different layers provided that the uncoded bit error rates of different layers are known. Moreover, we found the rate allocation for different SNRs.

The optimum rate allocation of the MLCM layers with 16-point ring constellation using the method in [Paper A] is shown in Fig. 1.6 for a distance $L = 5000$ km (the rest of parameters are the same as those in Section 4). This simulation confirms that the rate allocation for a non-Gaussian channel can show completely different behavior than a typical Gaussian channel. As seen, layer 1 is more vulnerable to errors at low SNRs while layer 3 needs more protection at high SNRs; this is different from results of Fig. 2.7 for a Gaussian channel.

Since the maximization of minimum Euclidean distance is not a valid criterion in the design of coded modulation for such a non-Gaussian channel, this design approach

significantly improves the performance of the system in comparison to traditional forward error correction methods.

Chapter 5

Conclusions and future work

The aim of this work is to design an efficient coded modulation scheme with regard to the spectral efficiency with an affordable complexity for a high data rate fiber-optical link. In order to achieve this goal, some contributions were introduced to be exploited in the design of such a system.

1 Conclusions

We proposed a new rate allocation scheme in [Paper A] for multilevel coded modulation (MLCM) based on an unequal error protection technique. The design criterion is to minimize the block error rate of the system, using a new method based on Lagrange multipliers. Since the BLER is computed by the union bound, this approach is suitable for moderate to high SNRs. The proposed method is simpler to implement than, e.g., the capacity design rule, and it shows up to 1 dB BLER performance improvement in comparison to previous known methods for moderate to high SNRs. In the new method, the rate allocation accounts for neighboring coefficients, Euclidean distances of the constellation, and the SNR of the system.

With special interest in fiber-optical channels, we elaborated on the performance of the MLCM scheme with a hard-decision multistage decoder. Moreover, to decrease the complexity of the MLCM scheme, an algorithm is proposed in [Paper B] with a multidimensional set partitioning method. This multidimensional MLCM shows better trade-off between performance and complexity for classical codes such as RS and BCH codes. The numerical results illustrate that for practical SNRs, we can design four-dimensional MLCM schemes with a lower complexity and a higher power efficiency than the one-dimensional systems.

In [Paper C], we presented the design of an MLCM scheme for a non-Gaussian fiber-optical channel with nonlinear phase noise. As discussed in Section 4, the channel distortion in the phase and amplitude of the transmitted signal are different. Therefore, an unequal error protection in the phase and radial direction is exploited to optimize the performance (BLER) of the system. It is shown that the new MLCM system can give better performance with lower complexity than independent error-correcting coding and modulation. Hence, the MLCM scheme provides the possibility of a reliable data transmission in a longer fiber or at a higher spectral efficiency.

Finally, in order to design a coded modulation scheme for a dual-polarization dispersion-managed fiber-optical link, statistics of the received signal are derived in [Paper D] for this channel. The derivations are performed for both lumped and distributed amplifications. These statistics consist of the pdf of the nonlinear phase noise and the joint probability density function of the received amplitudes and phases given the SNR of both polarizations. The numerical results for a specific system show 0.8 dB SNR penalty in utilizing a dual polarization scheme (to double the spectral efficiency) rather than a single polarization for 8-PSK, while this penalty is negligible for a QPSK constellation at SER $= 10^{-4}$.

2 Future work

As we addressed in [Paper A], one may generalize the proposed rate allocation method to a detector with soft-decision decoding. We will use the statistics of the dual polarization signal to design a coded modulation scheme based on the approach of [Paper C]. Moreover, one can introduce an accurate vector representation model (see Section 1) to derive the statistics of the received signal in a dispersion-managed fiber-optical channel. Finally, an important extension to [Paper D] can be the design of an ML receiver based on the derived statistics.

Bibliography

[1] C. Shannon, "A mathematical theory of communication," *Bell Systems Technical Journal*, vol. 27, pp. 379–423, 1948.

[2] R. Tkach, "Scaling optical communications for the next decade and beyond," *Bell Labs Tech. J.*, vol. 14, no. 4, pp. 3–9, Feb. 2010.

[3] R. J. Essiambre, G. Kramer, P. J. Winzer, G. J. Foschini, and B. Goebel, "Capacity limits of optical fiber networks," *J. Lightw. Technol.*, vol. 28, no. 4, pp. 662–701, Feb. 2010.

[4] J. L. Massey, "Coding and modulation in digital communications," *in Proc. of Int. Zurich Seminar on Digital Commun.*, pp. E2(1)–(4), Mar. 1974.

[5] G. Ungerboeck and I. Csajka, "On improving data-link performance by increasing channel alphabet and introducing sequence decoding," *in Proc. of IEEE Int. Symp. on Inform. Theory*, Ronneby, Sweden, June 1976.

[6] G. Ungerboeck, "Channel coding with multilevel/phase signals," *IEEE Trans. Inf. Theory*, vol. 28, no. 1, pp. 55–67, Jan. 1982.

[7] H. Imai and S. Hirakawa, "A new multilevel coding method using error correcting codes," *IEEE Trans. Inf. Theory*, vol. 23, pp. 371–377, May 1977.

[8] J. B. Anderson and A. Svensson, *Coded Modulation Systems.* Kluwer Academic/Plenum Publishers, 2003.

[9] J. G. Proakis and M. Salehi, *Digital Communications*, 5th ed. McGraw-Hill, 2008.

[10] S. Lin and D. J. Costello, Jr., *Error Control Coding*, 2nd ed. Prentice-Hall, 2004.

[11] P. Clarke and B. Honary, "Multilevel adaptive coded modulation waveforms for HF channels," *in Proc. of Int. Conf. on HF Radio Systems and Techniques*, pp. 240–243, 2003.

[12] S. Maeda, E. Sasaki, A. Ushirokawa, and Y. Koizumi, "Advanced SDH radio systems for transport of STM-1," *in Proc. of European Conf. on Radio Relay Systems*, pp. 349–354, Oct. 1993.

[13] "V.34: A modem operating at data signaling rates of up to 33 600 bit/s for use on the general switched telephone network and on leased point-to-point 2-wire telephone-type circuits," Feb. 1998. [Online]. Available: http://www.itu.int/rec/T-REC-V.34-199802-I/en

[14] L. Zhang and A. Yongacoglu, "Multilevel Reed–Solomon coding in asymmetric digital subscriber lines," *in Proc. of IEEE Symp. on Computers and Communications*, pp. 40–45, 2000.

[15] A. Calderbank, "Multilevel codes and multistage decoding," *IEEE Trans. Inf. Theory*, vol. 37, no. 3, pp. 222–229, Mar. 1989.

[16] G. D. Forney, Jr. and D. Costello, Jr., "Channel coding: The road to channel capacity," *Proceedings of the IEEE*, vol. 95, no. 6, pp. 1150–1177, 2007.

[17] U. Wachsmann, R. F. H. Fischer, and J. B. Huber, "Multilevel codes: theoretical concepts and practical design rules," *IEEE Trans. Inf. Theory*, vol. 45, no. 5, pp. 1361–1391, 1999.

[18] T. Lunn and A. Burr, "Number of neighbours for staged decoding of block coded modulation," *Electron. Lett*, vol. 29, no. 21, pp. 1830–1831, Oct. 1993.

[19] A. G. Burr and T. J. Lunn, "Block-coded modulation optimized for finite error rate on the white Gaussian noise channel," *IEEE Trans. Inf. Theory*, vol. 43, no. 1, 1997.

[20] G. D. Forney, Jr., M. Trott, and S. Y. Chung, "Sphere-bound-achieving coset codes and multilevel coset codes," *IEEE Trans. Inf. Theory*, vol. 46, no. 3, pp. 820–850, May 2000.

[21] G. J. Pottie and D. P. Taylor, "Multilevel codes based on partitioning," *IEEE Trans. Inf. Theory*, vol. 35, no. 1, pp. 87–98, Jan. 1989.

[22] R. Zamir, "Lattices are everywhere," *in Proc. of Int. Symp. on Inform. Theory and Its Applications*, pp. 392–421, Feb. 2009.

[23] J. H. Conway and N. J. A. Sloane, *Sphere Packings, Lattices and Groups*, 3rd ed. Springer-Verlag, NY, 1998.

[24] E. Agrell and M. Karlsson, "Power-efficient modulation formats in coherent transmission systems," *J. Lightw. Technol.*, vol. 27, no. 22, pp. 5115–5126, Nov. 2009.

[25] R. F. H. Fischer, *Precoding and signal shaping for digital transmission.* A John Wiley and Sons, Inc., 2002.

[26] L. Danzer, "Finite point-sets on S2 with minimum distance as large as possible," *Discrete Mathematics Archive*, vol. 60, no. 1–2, pp. 3–66, 1986.

[27] K. Ruotsalainen, "On the construction of the higher dimensional constellations," *in Proc. of IEEE Int. Symp. on Inform. Theory*, p. 490, 2002.

[28] G. D. Forney, Jr. and G. Ungerboeck, "Modulation and coding for linear Gaussian channels," *IEEE Trans. Inf. Theory*, vol. 44, no. 6, pp. 2384–2415, Oct. 1998.

[29] M. Tanahashi and H. Ochiai, "A multilevel coded modulation approach for hexagonal signal constellation," *IEEE Trans. Wireless Commun.*, vol. 8, no. 10, pp. 4993–4997, Oct. 2009.

[30] R. Hormis and X. Wang, "Low-complexity coded-modulation for ISI-constrained channels," *IEEE Trans. Commun.*, vol. 57, no. 6, pp. 1836–1846, 2009.

[31] G. D. Forney, Jr. and L.-F. Wei, "Multidimensional constellations. I. introduction, figures of merit, and generalized cross constellations," *IEEE J. Sel. Areas Commun.*, vol. 7, no. 6, pp. 877–892, Aug. 1989.

[32] G. D. Forney, Jr., "Multidimensional constellations. II. Voronoi constellations," *IEEE J. Sel. Areas Commun.*, vol. 7, no. 6, pp. 941–958, Aug. 1989.

[33] Y. Kofman, E. Zehavi, and S. Shamai, "Performance analysis of a multilevel coded modulation system," *IEEE Trans. Commun.*, vol. 42, no. 234, pp. 299–312, 1994.

[34] G. Caire, G. Taricco, and E. Biglieri, "Bit-interleaved coded modulation," *IEEE Trans. Inf. Theory*, vol. 44, no. 3, pp. 927–946, May 1998.

[35] T. M. Cover and J. A. Thomas, *Elements of information theory*, 2nd ed. New York: Wiley-Interscience, 2006.

[36] H. Imai and S. Hirakawa, "Correction to 'A new multilevel coding method using Error-Correcting codes'," *IEEE Trans. Inf. Theory*, vol. 23, no. 6, pp. 784–784, Nov. 1977.

[37] E. Zehavi, "8-PSK trellis codes for a Rayleigh channel," *IEEE Trans. Commun.*, vol. 40, no. 5, pp. 873–884, May 1992.

[38] A. Guillén i Fàbregas, A. Martinez, and G. Caire, "Bit-interleaved coded modulation," *Found. Trends Commun. Inf. Theory*, vol. 5, no. 1–2, pp. 1–153, 2008.

[39] ——, "Bit-interleaved coded modulation," *IEEE Trans. Inf. Theory*, vol. 44, no. 3, pp. 927–946, May 2008.

[40] R. H. Morelos-Zaragoza, M. P. C. Fossorier, S. Lin, and H. Imai, "Multilevel coded modulation for unequal error protection and multistage decoding — Part I. symmetric constellations," *IEEE Trans. Commun.*, vol. 48, no. 2, pp. 204–213, Feb. 2000.

[41] L. F. Wei, "Trellis-coded modulation with multidimensional constellations," *IEEE Trans. Inf. Theory*, vol. 33, no. 4, pp. 483–501, 1987.

[42] T. Kasami, T. Takata, T. Fujiwara, and S. Lin, "On multilevel block modulation codes," *IEEE Trans. Inf. Theory*, vol. 37, no. 4, pp. 965–975, 1991.

[43] T. Takata, S. Ujita, T. Kasami, and S. Lin, "Multistage decoding of multilevel block M-PSK modulation codes and its performance analysis," *IEEE Trans. Inf. Theory*, vol. 39, no. 4, pp. 1204–1218, 1993.

[44] K. O. Holdsworth, D. P. Taylor, and R. T. Pullman, "On the error performance of multilevel block-coded modulation," *IEEE Commun. Lett.*, vol. 3, no. 11, pp. 311–313, Nov. 1999.

[45] E. Hecht, *Optics*, 4th ed. Addison Wesley, 2001.

[46] G. P. Agrawal, *Nonlinear fiber optics*, 4th ed. Academic press, 2007.

[47] E. Ip and J. M. Kahn, "Compensation of dispersion and nonlinear impairments using digital backpropagation," *J. Lightw. Technol.*, vol. 26, no. 20, pp. 3416–3425, Oct. 2008.

[48] E. Ip, A. P. T. Lau, D. J. F. Barros, and J. M. Kahn, "Coherent detection in optical fiber systems," *Opt. Express*, vol. 16, no. 2, pp. 753–791, 2008.

[49] E. Ip and J. Kahn, "Digital equalization of chromatic dispersion and polarization mode dispersion," *J. Lightw. Technol.*, vol. 25, no. 8, pp. 2033–2043, Aug. 2007.

[50] S. J. Savory, G. Gavioli, R. I. Killey, and P. Bayvel, "Electronic compensation of chromatic dispersion using a digital coherent receiver," *Opt. Express*, vol. 15, no. 5, pp. 2120–2126, 2007.

[51] A. Demir, "Nonlinear phase noise in optical-fiber-communication systems," *J. Lightw. Technol.*, vol. 25, no. 8, pp. 2002–2032, Aug. 2007.

[52] S. Kumar, "Analysis of nonlinear phase noise in coherent fiber-optic systems based on phase shift keying," *J. Lightw. Technol.*, vol. 27, no. 21, pp. 4722–4733, Nov. 2009.

[53] J. P. Gordon and L. F. Mollenauer, "Phase noise in photonic communications systems using linear amplifiers," *Opt. Lett.*, vol. 15, no. 23, pp. 1351–1353, 1990.

[54] A. Mecozzi, "Probability density functions of the nonlinear phase noise," *Opt. Lett.*, vol. 29, no. 7, pp. 673–675, 2004.

[55] K.-P. Ho, "Probability density of nonlinear phase noise," *J. Opt. Soc. Am. B*, vol. 20, no. 9, pp. 1875–1879, 2003.

[56] ——, "Performance of DPSK signals with quadratic phase noise," *IEEE Trans. Commun.*, vol. 53, no. 8, pp. 1361–1365, Aug. 2005.

[57] G. Charlet, N. Maaref, J. Renaudier, H. Mardoyan, P. Tran, and S. Bigo, "Transmission of 40 Gb/s QPSK with coherent detection over ultra-long distance improved by nonlinearity mitigation," *in Proc. of European Conf. and Exhibition on Optic. Commun.*, 2006, Th4.3.4.

[58] C. Xu and X. Liu, "Postnonlinearity compensation with data-driven phase modulators in phase-shift keying transmission," *Opt. Lett.*, vol. 27, no. 18, pp. 1619–1621, 2002.

[59] K.-P. Ho, *Phase-Modulated Optical Communication Systems*. Springer, New York, 2005.

[60] A. P. T. Lau and J. M. Kahn, "Signal design and detection in presence of nonlinear phase noise," *J. Lightw. Technol.*, vol. 25, no. 10, pp. 3008–3016, Oct. 2007.

[61] M. Dlubek, A. Phillips, and E. Larkins, "Evolution of the probability density functions of Gaussian ASE noise in zero-memory nonlinear fiber," *Optical Fiber Technology*, vol. 15, no. 2, pp. 187–191, 2009.

[62] A. Mecozzi, "Limits to long-haul coherent transmission set by the Kerr nonlinearity and noise of the in-line amplifiers," *J. Lightw. Technol.*, vol. 12, no. 11, pp. 1993–2000, Nov. 1994.

[63] Y. Yadin, M. Orenstein, and M. Shtaif, "Statistics of nonlinear phase noise in phase modulated fiber-optic communications systems," *in Proc. of Optic. Fiber Commun. Conf.*, vol. 1, pp. 1800–1801, Feb. 2004, MF59.

[64] A. Bononi, P. Serena, and N. Rossi, "Modeling of signal-noise interactions in nonlinear fiber transmission with different modulation formats," *in Proc. of European Conf. and Exhibition on Optic. Commun.*, 2009.

[65] P. Serena, A. Orlandini, and A. Bononi, "Parametric-gain approach to the analysis of single-channel DPSK/DQPSK systems with nonlinear phase noise," *J. Lightw. Technol.*, vol. 24, no. 5, pp. 2026–2037, May 2006.

[66] G. Grimmett and D. Stirzaker, *Probability and Random Processes*, 3rd ed. Oxford University Press, 2001.

[67] K. P. Ho and J. M. Kahn, "Electronic compensation technique to mitigate nonlinear phase noise," *J. Lightw. Technol.*, vol. 22, no. 3, pp. 779–783, Mar. 2004.

[68] K. Kikuchi, M. Fukase, and S.-Y. Kim, "Electronic post-compensation for nonlinear phase noise in a 1000-km 20-Gbit/s optical QPSK transmission system using the homodyne receiver with digital signal processing," *in Proc. of Optic. Fiber Commun. Conf.*, Mar. 2007, paper OTuA2.

[69] A. J. Lowery, "Fiber nonlinearity pre- and post-compensation for long-haul optical links using OFDM," *Opt. Express*, vol. 15, no. 20, pp. 12 965–12 970, 2007.

[70] K. Roberts, C. Li, L. Strawczynski, M. O'Sullivan, and I. Hardcastle, "Electronic precompensation of optical nonlinearity," *IEEE Photon. Technol. Lett.*, vol. 18, no. 2, pp. 403–405, Jan. 2006.

[71] R. Waegemans, S. Herbst, L. Holbein, P. Watts, P. Bayvel, C. Fürst, and R. I. Killey, "10.7 Gb/s electronic predistortion transmitter using commercial FPGAs and D/A converters implementing real-time DSP for chromatic dispersion and SPM compensation," *Opt. Express*, vol. 17, no. 10, pp. 8630–8640, 2009.

[72] D.-S. Ly-Gagnon, S. Tsukamoto, K. Katoh, and K. Kikuchi, "Coherent detection of optical quadrature phase-shift keying signals with carrier phase estimation," *J. Lightw. Technol.*, vol. 24, no. 1, pp. 12–21, Jan. 2006.

[73] K. Kikuchi, "Phase-diversity homodyne detection of multilevel optical modulation with digital carrier phase estimation," *IEEE J. Sel. Topics Quantum Electron.*, vol. 12, no. 4, pp. 563–570, Jul. 2006.

[74] K. Sponsel, C. Stephan, G. Onishchukov, B. Schmauss, and G. Leuchs, "Nonlinear phase noise compensation using a modified nonlinear optical loop mirror," *in Proc. of Optic. Fiber Commun. Conf.*, Mar. 2010.

[75] K.-P. Ho and J. Kahn, "Electronic compensation technique to mitigate nonlinear phase noise," *J. Lightw. Technol.*, vol. 22, no. 3, pp. 779–783, Mar. 2004.

[76] C. Berrou, A. Glavieux, and P. Thitimajshima, "Near Shannon limit error-correcting coding and decoding: Turbo-codes." *in Proc. of IEEE Int. Conf. on Commun.*, vol. 2, pp. 1064–1070, May 1993.

[77] M. Magarini, R.-J. Essiambre, B. E. Basch, A. Ashikhmin, G. Kramer, and A. J. de Lind van Wijngaarden, "Concatenated coded modulation for optical communications systems," *IEEE Photon. Technol. Lett.*, vol. 22, no. 16, pp. 1244–1246, Aug. 2010.

[78] Y. Cai, J. M. Morris, T. Adali, and C. R. Menyuk, "On turbo code decoder performance in optical-fiber communication systems with dominating ASE noise," *J. Lightwave Technol.*, vol. 21, no. 3, pp. 727–734, Mar. 2003.

[79] I. Djordjevic, M. Arabaci, and L. Minkov, "Next generation FEC for high-capacity communication in optical transport networks," *J. Lightw. Technol.*, vol. 27, no. 16, pp. 3518–3530, Aug. 2009.

[80] M.-S. Kao, H.-Y. Chen, and D. Lin, "A product-coded WDM coding system," *IEEE Trans. Commun.*, vol. 44, no. 1, pp. 43–46, Jan. 1996.

[81] W. E. Ryan and S. Lin, *Channel Codes: Classical and Modern.* Cambridge University Press, 2009.

[82] E. Arikan, "Channel polarization: A method for constructing capacity-achieving codes for symmetric binary-input memoryless channels," *IEEE Trans. Inf. Theory*, vol. 55, no. 7, pp. 3051–3073, 2009.

[83] R. Gallager, "Low-density parity-check codes," *IRE Trans. on Inf. Theory*, vol. 8, no. 1, pp. 21–28, Jan. 1962.

[84] G. Bosco and S. Benedetto, "Soft decoding in optical systems: Turbo product codes vs. LDPC codes," *Optical Commun. Theory and Techniques*, pp. 79–86, 2005.

[85] M. Kumar, "Asynchronous BPPM OCDMA systems with trellis-coded modulation," *IEE Proceedings Optoelectronics*, vol. 151, no. 4, pp. 193–201, Aug. 2004.

[86] J. Kahn, "Modulation and detection techniques for optical communication systems," *Optical Amplifiers and Their Applications/Coherent Optical Technologies and Applications*, p. CThC1, 2006.

[87] G. Liva, S. Song, L. Lan, Y. Zhang, S. Lin, and W. E. Ryan, "Design of LDPC codes: A survey and new results," *J. Commun. Softw. Syst.*, vol. 2, no. 3, pp. 191–211, 2006.

[88] S. Lotz, W. Sauer-Greff, and R. Urbansky, "Iterative demapping and decoding for bit-interleaved coded modulation in optical communication systems," *in Proc. of Int. Conf. on Transparent Optic. Networks*, 2010.

[89] I. Djordjevic, M. Arabaci, and L. Minkov, "Next generation FEC for high-capacity communication in optical transport networks," *J. Lightw. Technol.*, vol. 27, no. 16, pp. 3518–3530, Aug. 2009.

[90] H. Zhao, E. Agrell, and M. Karlsson, "Trellis-coded modulation in PSK and DPSK communications," *in Proc. of European Conf. and Exhibition on Optic. Commun.*, 2006.